

# Effect of temperature history on the mechanical behaviour of a filler-reinforced NR/BR blend: literature review and critical experiments

A. F. M. S. Amin<sup>1,\*</sup>, A. Lion<sup>2</sup>, and P. Höfer<sup>2</sup>

<sup>1</sup> Department of Civil Engineering, Bangladesh University of Engineering and Technology, Dhaka 1000, Bangladesh

<sup>2</sup> Institute of Mechanics, Faculty of Aerospace Engineering, University of Federal Armed Forces Munich, 85577 Neubiberg, Germany

Received 17 September 2009, accepted 1 February 2010

Published online 23 April 2010

**Key words** Mullins effect, healing, strain rate effect, crystallization, melting.

The influence of the temperature history on the Mullins effect, its recovery behaviour and the rate dependence is experimentally investigated using NR/BR (NR: natural rubber, BR: polybutadiene rubber) rubber blend. The crystallization which occurs in rubber during long term storage below the melting temperature has been taken into account to interpret the experimental data. To study the influence of low temperatures and large deformations on the Mullins effect, cyclic strain-controlled processes are applied under different temperatures. The softened specimens are subjected to a sequence of heating, cooling, and conditioning processes in order to study the influence of the temperature history on healing, melting, and recrystallization. The results indicate the existence of a threshold temperature: if the specimen temperature is larger than this threshold, a nearly complete recovery of the material occurs within finite time, while any temperature below this limit will be too small for healing. The temperature dependence of both the healing and the Mullins effect in rubber with different degrees of crystallinity is resolved by considering the melting and recrystallization rates. The rate dependence of the blend is investigated under different temperatures via monotonic and cyclic tension tests at different strain rates and relaxation tests. The experimental data suggests a decrease in the strain rate sensitivity at higher temperatures.

© 2010 WILEY-VCH Verlag GmbH & Co. KGaA, Weinheim

## 1 Introduction

### 1.1 General

Filler-reinforced vulcanized rubber and its blends are frequently-used for engineering applications for over a century (cf. Morawetz [1]). Traditional applications include tires, seals, bushings, and engine mounts. Some specially-vulcanized types of rubber, called high damping rubber (HDR), are used to construct base isolation bearings that protect buildings, bridges, or other sensitive systems from destructive excitations (see, e.g., Kelly [2]). The use of rubber for air springs of luxury cars, for acoustic coatings of sonar transducers of submarines (see Roland [3]), and for biomedical applications is common practice. To shape the geometry of these products, geometric nonlinearities need to be considered together with the mechanical properties of the material. The application of a numerical procedure which considers an adequate constitutive model founded on nonlinear continuum mechanics and the principles of thermodynamics (c.f. Haupt [4]) can bring realistic sophistication to a computer aided design and manufacturing process.

The mechanical behaviour of filler-reinforced rubber originates from a network of macromolecules containing chemical and physical crosslinks, entanglements and filler particles (c.f. Blümmler and Blümich [5], Bergström and Boyce [6, 7], Amin et al. [8, 9] for various imaging techniques that can ascertain chemical composition, filler matrix interaction, filler dispersion, and morphology of rubber macromolecules). The macromolecular network of filler-reinforced rubber exhibits rate-dependent behaviour, hysteresis and energy dissipation during monotonic and cyclic deformations. Therefore, the stress response of this material depends strongly on the applied deformation history (Treloar [10]). Lion [11–13] provided experiments and a constitutive model which also considers the temperature. On the other hand, macromolecular networks can change their microstructure at temperatures much higher than cryogenic temperatures (200 K). Such processes are possible in two different ways: 1) the healing of Mullins effect (c.f. Bueche [14]) and 2) the crystallization process (c.f. Wood and

\* Corresponding author E-mail: amin@bdcom.com, samin@ce.buet.ac.bd, Telephone: +880-2-9671155, Fax: +880-2-9665639

Roth [15]; Wood and Bekkedahl [16]; Gent [17]; Stevenson [18]; Gent and Zhang [19]; Fuller et al. [20]). Both the temperature and the deformation history are the determining factors for the duration needed to complete these changes. The time-, temperature-, and deformation-dependent changes in the macromolecular network, however, influence the mechanical material behaviour of rubber. Thus, there exists an obvious necessity to extend the experimental knowledgebase of the material over the practical deformation and temperature ranges such that motivations for founding more general constitutive models can be obtained. To this end, this paper examines the available literature that documents the behaviour of rubber when it is subjected to thermo mechanical processes. In this course, the thermal history dependence of the mechanical behaviour of NR/BR (NR: natural rubber, BR: polybutadiene rubber) blend is experimentally investigated to point out the limitations of the current understanding on developing constitutive models considering these phenomena.

## 1.2 Fundamental mechanical phenomena in vulcanized rubbers

When a virgin rubber is subjected to a cyclic deformation process, a stress softening phenomenon, commonly known as the Mullins effect [21–26], occurs during the first few cycles. Fig. 1 illustrates this effect when a virgin specimen is subjected to a cyclic process with different maximum stretches  $\lambda_1, \lambda_2, \lambda_3,$  and  $\lambda_4,$  respectively. The softening, occurring between cycles 10 and 11 in a virgin rubber at the stretch level  $\lambda_4,$  is illustrated in Figs. 1b and 1c. It increases progressively when the material experiences larger stretch amplitudes, e.g.  $\lambda_1 < \lambda_2 < \lambda_3 < \lambda_4.$  At any amplitude lower than the past maximum amplitude, the material exhibits a repeatable stress-strain response with a very little softening in the successive cycles (Lion [11], Gentot et al. [27]). The effect is observed in unfilled rubber, filled rubber vulcanisates, and in also various soft biological tissues, e.g. human brain (Krishnaswamy and Beatty [28], Franceschinia et al. [29]). In unfilled rubber, the stress softening is attributed to the retarded response of network chains due to viscous drag exerted by neighbouring molecular chain segments whereas in filled rubbers the breakdown of interactions between filler particles and between filler and rubber provide additional source of softening (c.f. Mullins [25], Beatty and Krishnaswamy [30] and the references cited therein).

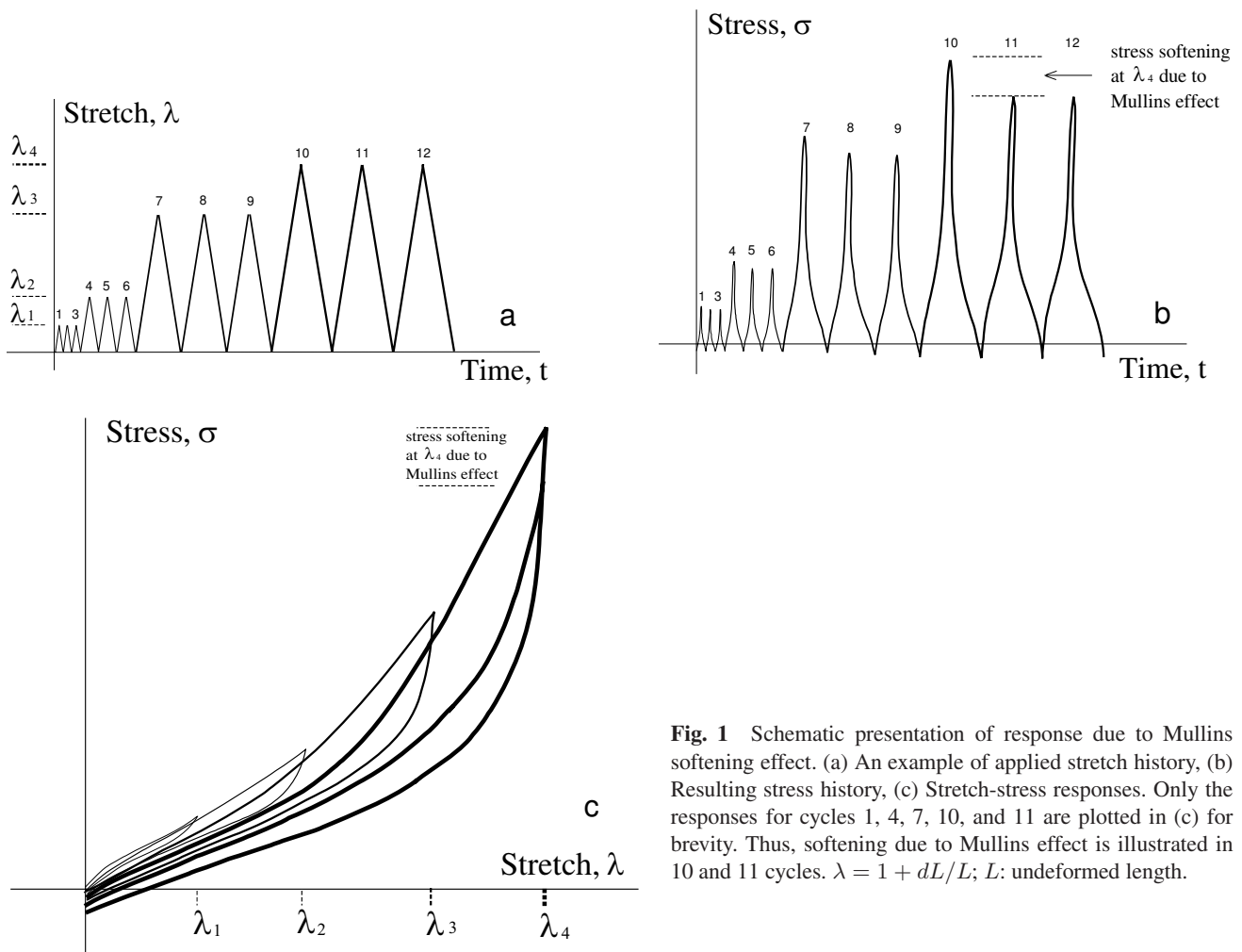


**Fig. 1** Schematic presentation of response due to Mullins softening effect. (a) An example of applied stretch history, (b) Resulting stress history, (c) Stretch-stress responses. Only the responses for cycles 1, 4, 7, 10, and 11 are plotted in (c) for brevity. Thus, softening due to Mullins effect is illustrated in 10 and 11 cycles.  $\lambda = 1 + dL/L$ ;  $L$ : undeformed length.

As we know, the stress response of rubber contains a characteristic nonlinearity (Treloar [31]) and depends significantly on the strain rate (Greensmith [32]; Gent [33, 34]). Fig. 2 depicts that the stress increases with the increase of the strain rate. However, in viscoelasticity there are two limiting stress-strain curves: the instantaneous response and the equilibrium response ('x' and 'y' in Fig. 2). They are obtained under infinitely fast and infinitely slow strain rates. Furthermore, the stress responses of filler-reinforced rubber differ significantly between loading and unloading due to hysteresis effects; the strain rate sensitivity is weaker during unloading than that during loading. Lion [11], Bergström and Boyce [6, 35], Miehe and Keck [36], Haupt and Sedlan [37] report more information on the strain rate dependence of filler-reinforced rubber via monotonic experiments and relaxation tests (Figs. 2–3). Bergström and Boyce [6, 35] further clarify the relationship between the filler content and its influence on the rate dependence. Amin et al. [8, 38] review recent works on the strain rate dependence of elastomers. In their experiments, they show that the rate of stress relaxation of filler-reinforced rubber is logarithmically related to the deformation at which the relaxation occurs. From these observations, mostly conducted at room temperature ( $\sim 293$  K), there comes out a consensus that the stress relaxation and the rate-dependence are related to readjustments or reorientations of the macromolecules. Under stress, the molecular chains within the rubber slide. Relaxation corresponds to intermolecular slippage and is accompanied by reversible breaking or swapping of weak physical bonds. Various types of readjustments or molecular slippage mechanisms should be distinguished and have their own relaxation times. Relaxation on a local scale is very short and the relaxation time on the long term scale can be quite long. Since there is a large range of different molecular chain lengths and readjustment mechanisms in rubber, there is a large or continuous range of relaxation times. Studies of relaxation phenomena of different polymers are available in Khan and Zhang [39] and Krempl and Khan [40]. Yu and Selvadurai [41] interpret the origin of rate dependence in such a polymer network due to the formation and orientation of 'crystallite transient' within the polymer.

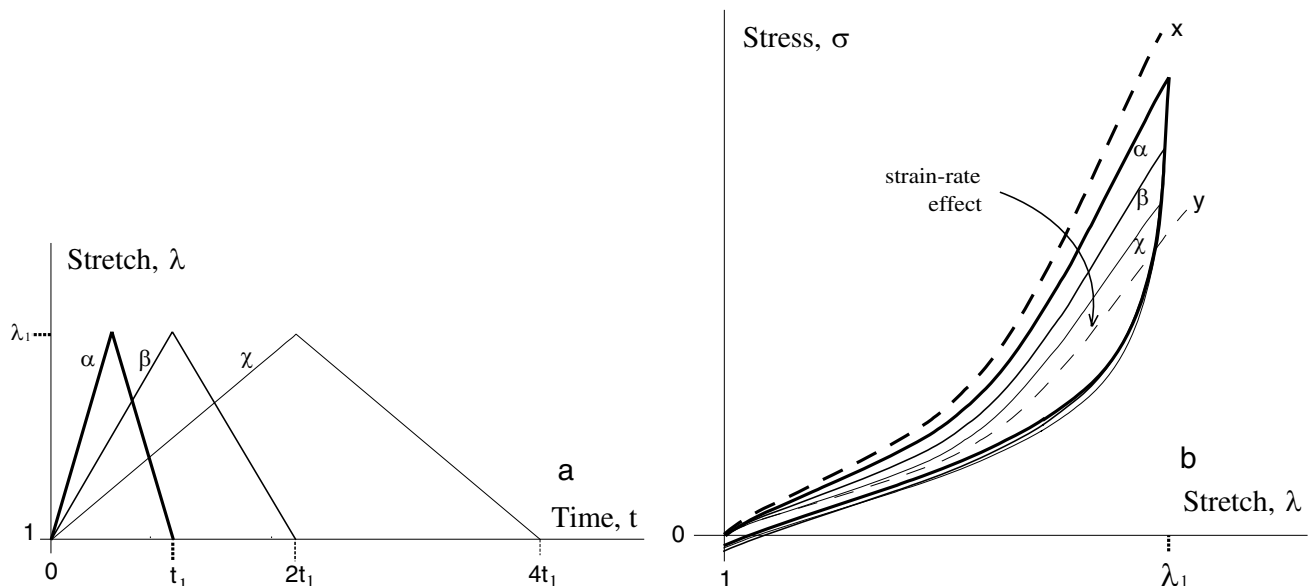


**Fig. 2** Schematic presentation of strain rate effect in cyclic tension. (a) An example of applied stretch histories, (b) Resulting stretch-stress responses.

### 1.3 Effect of temperature

Available experimental data of the mechanical behaviour of rubber is mostly related to isothermal conditions. The temperature dependence of rubber is due to two different phenomena. The first phenomenon, the Gough-Joule effect, is determined by the entropy elasticity, whereas the second effect is caused by inelastic energy dissipation or hysteresis [42]. In dependence on both the loading history and the boundary conditions, the resulting process can be isothermal, adiabatic, or in-between these limit cases. The process is adiabatic, if a rubber component has either a large geometry or the deformations are applied with a sufficient fast rate (Lion [13]). This is a concern in many technical applications, for example, in base isolation bearings consisting of several layers of metal sheets and rubber. The rubber layers of these bearings experience a quasi-adiabatic process when stochastic excitations are applied. Thus, they induce pronounced temperature increases (Gent and Hindi [43]). On the other hand, a rubber product is often exposed to temperature changes over its service life due to variations of the ambient temperatures. The climatically-induced temperature range of base isolation bearings is between

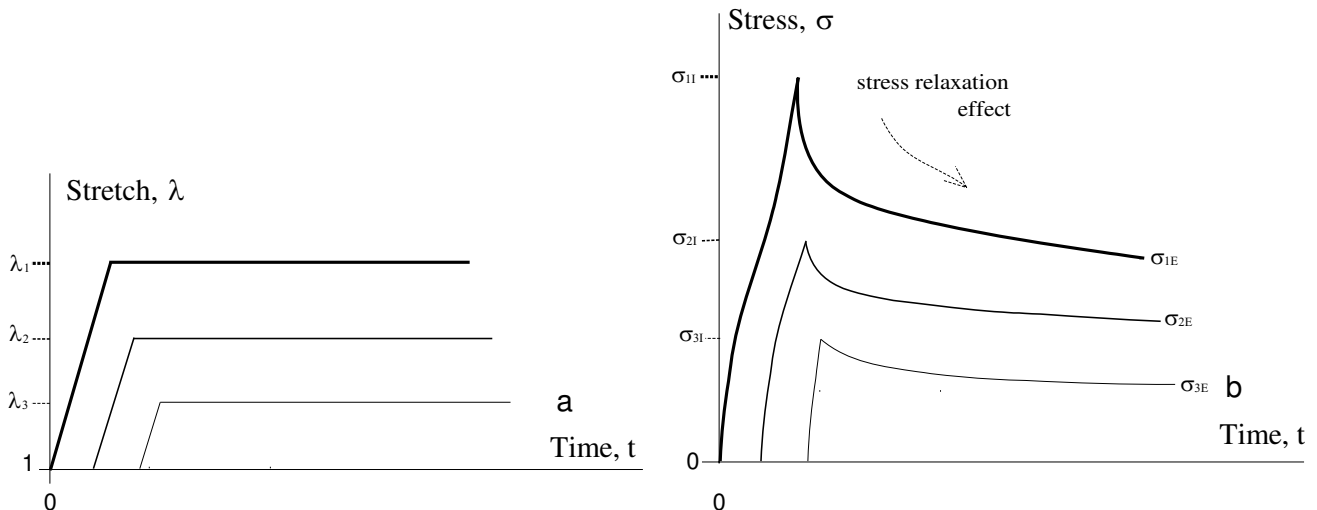


**Fig. 3** Schematic presentation of stress relaxation phenomena at different magnitudes of cyclic tension. (a) An example of applied stretch histories, (b) Resulting stress histories. Stress relaxes from  $\sigma_{iI}$  to  $\sigma_{iE}$  due to strain rate effect induced by viscosity.

250 K to 320 K (Yakut and Yura [44, 45]; Fuller et al. [20]). In this sense, aircraft tires are subjected to large temperature variations not only during storage, but also during the takeoff and landing phases (Roland [3], Park et al. [46]) due to inelastic energy dissipation. The temperature can reach values of about 370 K or even more. However, the temperature ranges that rubber products are usually subjected to lie well between two limits, namely the glass transition temperature,  $T_g$  (Smith [47]) and the chemo-rheological temperature,  $T_{cr}$  (Lin et al. [48], Shaw et al. [49], Wineman and Shaw [50]). At temperature values below  $T_g$  the mobility of the macromolecules decreases significantly while at temperatures above  $T_{cr}$  the macromolecular system undergoes time- and temperature-dependent irreversible changes and evolves into a new material system with reduced stiffness [50]. A change in the temperature within the boundaries  $T_g$  and  $T_{cr}$  primarily leads to a change in the internal energy density and results in a faster movement of the macromolecules. In the current essay we restrict our experiments, interpretations, and discussion within these two boundaries.

### 1.3.1 Mullins softening effect and healing

Changes in the structure of macromolecular networks due to changes in the temperature and their effect on the mechanical material behaviour are discovered when Bueche [14] made the striking report that the Mullins effect can recover when softened rubber is stored at a temperature of about 373 K for a few hours. Soos [51], Drozdov and Dorfmann [52] later on supported this proposition. They were able to restore the initial properties of preloaded rubber samples after storing the specimens at 373 K–393 K for a few hours. This implies a characteristic reversibility of the Mullins effect upon a thermal input. Nevertheless, the temperature range (373 K–393 K) for this metamorphosis lies inside the service temperature range of many rubber products. Govindjee and Simo [53–55], Johnson and Beatty [56, 57], Lion [11], Ogden and Roxburgh [58], Beatty and Krishnaswamy [30, 59], DeSimone et al. [60], Moshev et al. [61], Besdo and Ihlemann [62, 63], Diani et al. [64] interpret the Mullins effect from the viewpoint of damage mechanics. This interpretation is based on the original proposal provided by Mullins and Tobin [65] to formulate models that describe the softening effect under isothermal conditions. Horgan et al. [66] also developed a theory to describe the Mullins effect in rubber-like solids. Their theories are related to the idea of changing natural configurations (Rajagopal and Wineman [67]) and to pseudo-elasticity (Ogden and Roxburgh [58]). On the other hand, Yeoh [68], Yamashita and Kawabata [69], Lion [11], Bergström and Boyce [35], Miehe and Keck [36], Amin et al. [8, 38] apply a specified preloading history with a constant maximum strain amplitude on the virgin specimen to ‘remove’ the Mullins effect from the respective phenomena of interest. This method is applied at room temperature and assumes the existence of a certain amount of irreversible damage in the specimen due to the preloading process. On the one hand, this approach allows investigating the effects of interest like relaxation, rate-dependence or hysteresis. On the other hand, the reversible nature of the Mullins effect as indicated by Bueche [14], Soos [51], or Drozdov and Dorfmann [52] is in contradiction to the assumption of irreversible damage (cf. Chagnon et al. [70]). To the knowledge of the authors, there is no experimental information on the change in the stress response or the stress-strain behaviour due to heat treatment of preloaded rubber specimens.

### 1.3.2 Temperature/time induced and deformation/stress induced crystallization process

The macromolecular network of rubber can locally transform from the amorphous to the crystalline state. This phase transformation is either a temperature induced (Wood and Roth [15]; Wood and Bekkedahl [16]) or a deformation-induced (Wood and Roth [15]; Gent [17]; Tobolsky and Brown [71]; Kraus and Gruver [72]; Wasiak [73]; Mitchell and Meier [74]; Gent and Zhang [75]) crystallization process. There is also a reverse transformation, known as melting, when the deformation is reduced or the temperature is increased. Stevenson [18] characterizes the crystallization process in terms of three properties: induction period, growth rate and the equilibrium state. It is resolved that the induction period of the crystallization process in natural rubber increases with decreasing strain. With decreasing temperature, it passes through a broad minimum at about 248 K. Stevenson notices that at zero deformation, the rate of crystallization slows down significantly above a temperature of 298 K whereas melting processes are initiated above the melting temperature. Thus, the attainment of the equilibrium state of crystallization is closely related to both the temperature and the deformation history.

Wood and Bekkedahl [16], Gent [17], and Fuller et al. [20] quantified the crystallization process by measuring the volume change in natural rubber (NR) and high damping natural rubber (HDNR). Lee and Singleton [76] used the differential scanning calorimetry (known as DSC) technique to identify the onset temperatures for exothermic crystallization and endothermic melting processes (see also Gent and Zhang [19] on BR). Luch and Yeh [77] observed strain induced crystallization in NR via electron microscopy. Very recently, Toki et al. [78, 79] and Poompradub et al. [80] used the real-time wide angle X-ray diffraction technique on NR, synthetic poly-isoprene rubber (IR) and BR specimens to study the strain induced crystallization mechanisms. These studies reveal that crystal formation and melting due to thermal or mechanical loads influence the material behaviour of rubber. Toki et al. [78] interpret the hysteresis properties observed in the mechanical stress-strain responses as strain induced crystallization and amorphisation. However, the strain rate dependence, the stress relaxation and the hysteresis on the ambient temperature and the temperature history is yet to be investigated via comprehensive experiments.

Recent theoretical works (c.f. Lion [11]; Bergström and Boyce [35]; Bonet [81]; Laiarinandrasana et al. [82]; Amin et al. [8, 38]) model the rate-dependent behaviour of rubber only under isothermal conditions at room temperature and do not address any aspect related to crystallization. In contrast, Lion [13] measured the temperature dependence of the strain rate effect of carbon black-filled vulcanisates through a series of monotonic tests in tension and compression conducted at different temperatures (253 K–373 K) and strain rates ( $2 \times 10^{-1} \text{ s}^{-1}$ – $2 \times 10^{-4} \text{ s}^{-1}$ ). All tests were conducted with virgin specimens without any mechanical preloading. The stress responses at different temperatures include some additional changes in the stiffness due to the Mullins effect. In his tests, Lion observed more pronounced rate sensitivity in combination with longer relaxation times at temperatures below 273 K together with a marked increase at 253 K. The test data between 296 K and 373 K suggests weaker hysteresis behaviour at higher temperature levels. However, these measurements were neither aimed to study the cyclic material behaviour below 296 K nor to study the effect of the temperature history on the stress-strain behaviour. Other investigations of the temperature and strain rate dependence of polymeric materials are reported in Khan et al. [83] for Adiprene-L100 and in Khan and Farrokh [84] for Nylon 101. These studies consider neither crystallinity-related effects nor the influence of the temperature history. Fuller et al. [20] suggests tempering the specimen at an elevated temperature to remove the crystallization that may occur during long term storage. However, it is important to know how such a pre-tempering process affects the mechanical material behaviour. Escandar et al. [85] report about the change in the shear modulus of preloaded HDR at different temperatures and strain rates. Yet, the experimental work neither covers the relaxation behaviour nor the effect of temperature history on the material. Flory [86, 87], Evans et al. [88], Roberts and Mandelkern [89] attempted to explain the crystallization phenomena from principles of thermodynamics and experimental data available at that time. Other theoretical descriptions of crystallization can be found in Ziabicki [90–92], Ziabicki and Sajkiewicz [93]; Negahban [94–97]. Through these works, it was possible to describe the effect of temperature on the nonlinear monotonic responses of NR together with crystallization effects. Kannan and Rajagopal [98] and Kannan et al. [99] provide a theoretical framework to study the deformation induced crystallization and describe the solidification of polymer melts related to fibre spinning. Although such a framework is quite general in nature, no attempt is known to extend such an approach to study crystallization in viscoelastic solids e.g. filled rubbers. Not to mention, the limited availability of experimental information on the effect of crystallinity on both the equilibrium and the rate-dependent mechanical behaviour of filled rubber retarded such promising theoretical developments.

### 1.4 Current objectives

The current work studies the thermo mechanical behaviour of a NR/BR blend which is prone to crystallization (Sect. 2.1). The specimens are tested under tension to understand the effect of the temperature on the mechanical behaviour of the blend. In this course, we apply a specified deformation history on a virgin specimen at a reference temperature and reapply the same deformation history at that reference temperature for a few more times, but also after subjecting the specimens to various temperature histories (Sect. 2.3). By this sequence of events, an insight into the thermo rheological processes

which occur in the material can be obtained. In this way, the temperature history dependences of the Mullins effect and its healing, the stress-strain responses, the rate dependence, and the hysteresis behaviour are investigated under five reference temperatures (Table 1). The limitations of the current approaches to model the material behaviour are discussed on the basis of the test results. In addition, some hints are offered to formulate models with improved prediction capability. The next part of the paper begins by explaining the experimental procedure together with the observations related to the Mullins effect and healing phenomena due to tempering. The rate dependence phenomena in the virgin and the tempered specimens are addressed in the later sections.

## 2 Experimental procedure

The discussion presented in Sect. 1 reveals the lack of experimental information on the effect of temperature on the constitutive phenomena observed in rubber. With this end in view, the developed test procedure was tailored to investigate the changes in the mechanical material behaviour (Sect. 1.2) of rubber due to temperature history effects. The specimens were subjected to specified deformation processes at different temperatures. Comparisons were made between the stress responses obtained from a particular deformation process under different specimen temperatures. The experimental strategy also considers the process dependence of the mechanical responses. This effect is eliminated by applying the same deformation process in terms of maximum strain amplitude, strain rate, and duration. The ambient temperature is taken as the only variable parameter.

### 2.1 Specimens

All tests were carried out with specimens made of an NR/BR blend. The constituents of the blend NR and BR were independently studied in the past for investigating the crystallization process (Sect. 1.3.2 and the references cited therein, ASTM D 832-92 [100], Chenal et al. [101], Gent and Zhang [19]). Different procedures for blending and vulcanization together with information about the macromolecular and topological structure of the blend are available elsewhere (c.f. Yehia et al. [102], Jurkowska et al. [103, 104], Likožar and Krajnc [105], Palaty and Joseph [106]). The filler-reinforced NR/BR blend described in this paper was prepared by the Lord Corporation ([www.lord.com](http://www.lord.com)) in 2004, following a recipe for use in the bearings of helicopters. After vulcanization, some of the specimens were tested at 293 K in the framework of a doctoral dissertation in 2004 of Heimes [42], while the others were stored in an opaque cardboard box under clean and air-conditioned laboratory conditions for three years at 296 K and 50% relative humidity. The tests reported in this essay were conducted in February 2007. The stored specimens are referred as the virgin specimen in the rest part of this paper.

To illustrate the crystallization and melting phenomena in more detail, DSC tests (Fig. 4) were carried out with both virgin specimens and specimens after application of thermal histories. In the DSC curves (Fig. 4a) an exothermal event can be noted in between 260 K–280 K and an endothermic event in between 312 K–344 K. These two temperature ranges can be interpreted as the ranges where crystallization and melting processes can proceed, respectively, at a fast rate (Sect. 1.3.2). By comparing all the curves (Fig. 4), it is seen that a DSC signal, therefore the heat capacity of the sample generally gets reduced upon tempering at a temperature above the range of melting (312 K–344 K) and increases upon quenching within the crystallization temperature range (260 K–280 K). Finally, we note further that the melting peak reappears weakly in the tempered sample (Fig. 4a, Heating run 2) and strongly in the quenched sample (Fig. 4b, Heating run 4) indicating the thermal history dependence of the crystallization and melting phenomena. The DSC data thereby clarifies the existence of crystallization-melting effects in the specimen and, that the temperature (296 K) at which the specimens were stored for the duration of three years (2004–2007) lies below the melting temperature of the material (see also Sect. 1.3.2 and the references cited therein). The glass transition temperature  $T_g$  of the sample was measured via DSC to be 210 K whereas thermo gravimetric analysis (TGA) has shown that the specimens thermally degrade at temperatures above 493 K.

### 2.2 Testing machine and data acquisition

The experiments were conducted using a computer-controlled electro mechanic testing machine (Zwick Roell Z20, [www.zwick.com](http://www.zwick.com)) using a 20 kN load cell (Gassmann Theiss Messtechnik 45829). The NR/BR specimens used in this experiment were cylindrical in shape (25 mm in diameter and 50 mm in length). 25 mm thick steel flanges were vulcanized to the ends of the specimens in order to grip them with the X-bars of the testing machine to test under tension. The maximum displacement rate of the testing system is about 17 mm/s. The displacement rate of the testing machine was controlled by the displacement rate of the X-bar. In order to maintain a constant specimen temperature, a computer controlled temperature chamber with an accuracy of  $\pm 1$  K was used. The force was recorded from the load cell and long-way extensometers were used to measure the diametral strain at the mid-height of the specimen. Thus, the cross sectional areas of the stretched

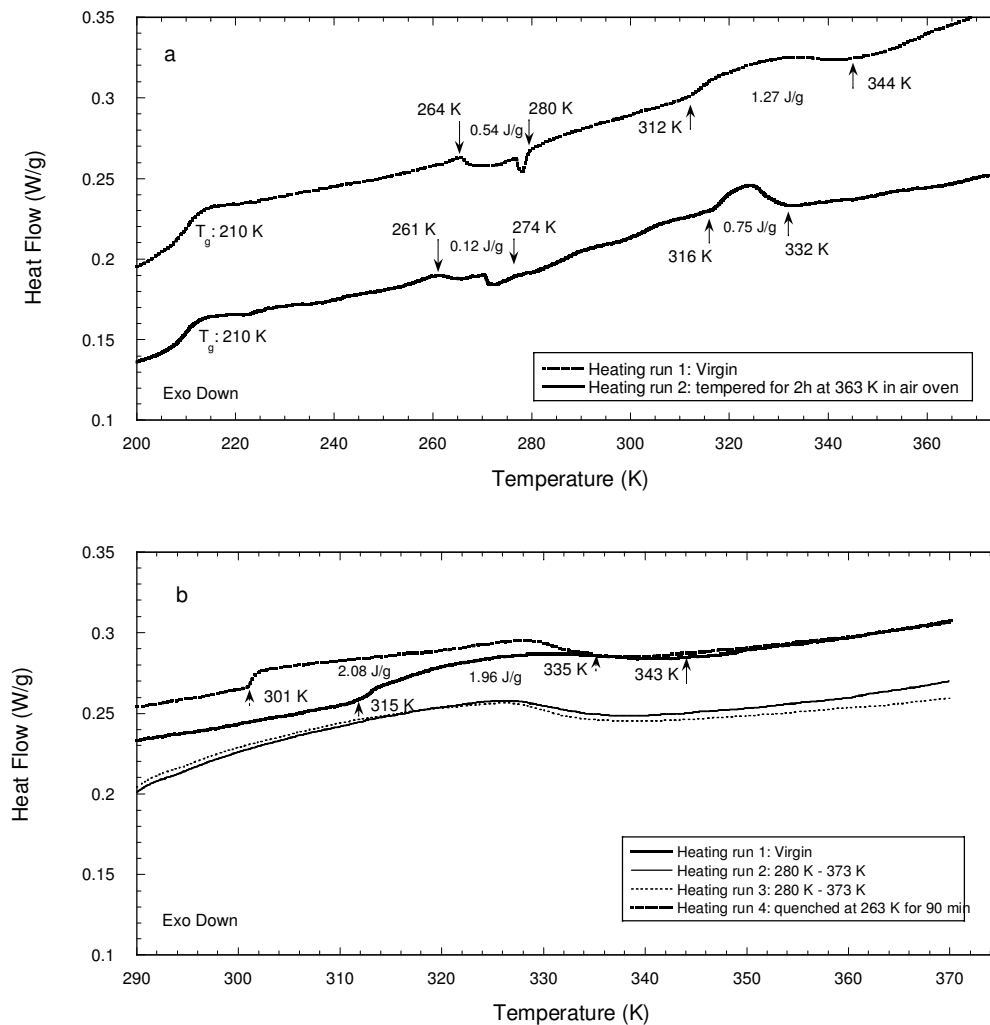


**Fig. 4** DSC curves of the specimen in virgin condition and after application of different thermal histories are presented. To obtain the DSC curves, the virgin sample was encapsulated in aluminium pan and mounted in the DSC machine (TA Instruments Model Q10) at room temperature and cooled down using liquid nitrogen. The sample was then heated up at a rate of 10 K/min in dry nitrogen environment. (a) Heating run 1: the virgin sample was cooled to about 40 K below the anticipated  $T_g$  and then heated up to 373 K. After finishing the first run, the sample was tempered for 2 h in an air oven (outside the DSC chamber) at 363 K and the DSC test was repeated (Heating run 2). The duration the specimen experienced below 310 K after tempering is about 30 min. (b) Heating run 1: a new virgin sample was mounted and cooled to about 40 K below the anticipated  $T_g$  and then heated up to 375 K. Heating run 2: After the end of heating run 1, the sample was equilibrated at 280 K. The temperature lies just above the detected temperature range (260–280 K) where an exothermic process was observed to take place (Fig. 4a). The sample was heated up to 373 K. Heating run 3: Heating run 2 was repeated once again. Heating run 4: Just after the end of Heating run 3, the sample was preserved for 90 min at 263 K ( $\pm 2$  K) in the DSC chamber and then heated up to 373 K.

specimens, measured at the mid-height, were used to calculate the Cauchy stress. The prescribed temperature history was also recorded.

### 2.3 Applied temperature and deformation histories

Both the temperature and the deformation history applied to the virgin specimens are summarized in Figs. 5 and 6. The specimen temperatures ( $T$  K) had five reference values in the range between 253 K and 333 K (Table 1). Further details of the deformation histories are documented in Table 2. To ensure that a particular specimen experiences only one temperature history, a new virgin specimen was used for each reference temperature. To ensure a homogeneous temperature distribution

of  $T$  K in the specimen before driving the mechanical tests (Fig. 6) at *II, V, VIII, XI, XIV* segments of the temperature history (Fig. 5), the specimen was first mounted in the temperature chamber at room temperature ( $\sim 293$  K) and allowed to heat up (or to cool down) under load-free conditions. During this process, the specimens were allowed to change their length under stress-free conditions. The attainment of the thermal equilibrium was assured from the asymptotic convergence of the temperature induced elongation or contraction of the specimen. Temperature preconditioning of a duration of 60 minutes before initiating the actual mechanical test procedure was long enough to attain the thermal equilibrium state.

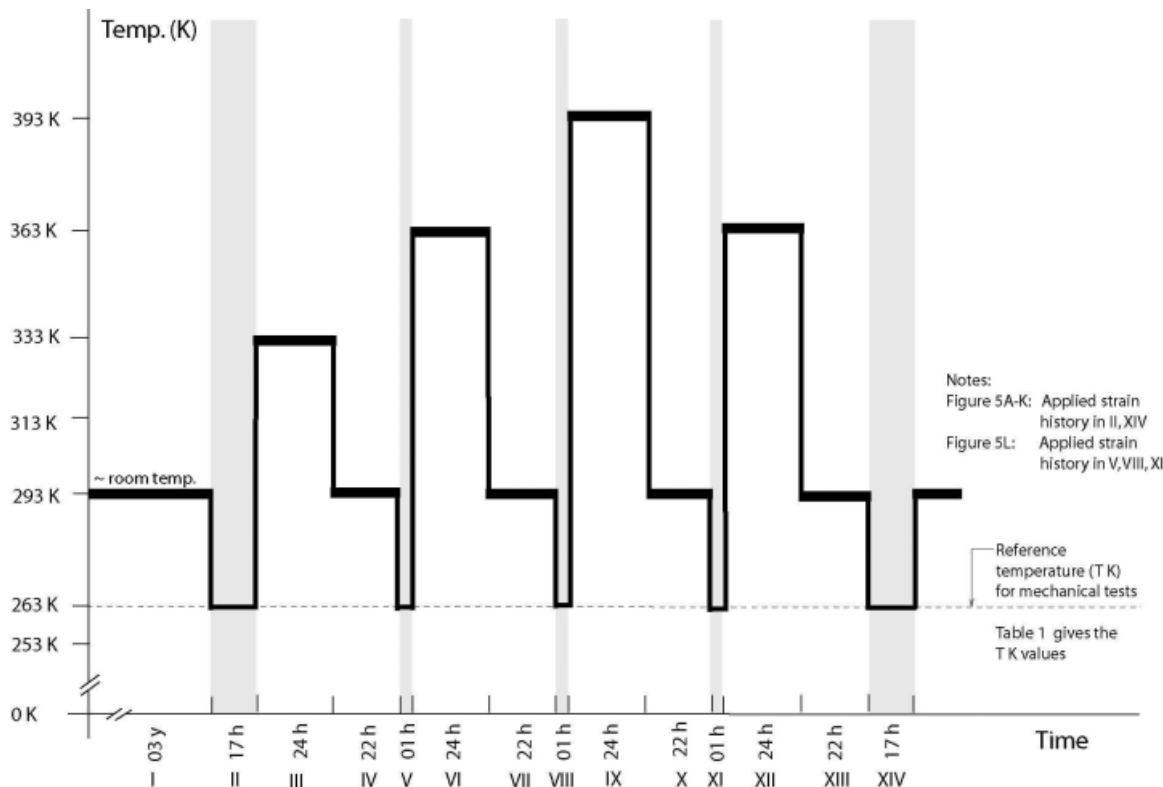


**Fig. 5** Temperature histories applied to specimens. The figure is to be read in conjunction with Fig. 6, Tables 1 and 2.

**Table 1** Reference temperatures (Fig. 5) for mechanical tests.

Sl. no.	Reference temperatures $T$
1	253 K
2	263 K
3	293 K
4	313 K
5	333 K

Note: The Table is to be read in conjunction with Figs. 5 and 6, and Table 2.

The mechanical test procedure applied to a specimen at a temperature level of  $T$  K is presented in Fig. 6. It contains twenty cyclic segments as depicted in subfigures a–l. Between each segment of the cyclic process (a–k), a hold time of 1500 s was applied to allow the regularization of the stress relaxation that occurs between the tests. However, the force levels were continuously recorded during this hold time to correct the recorded data. The maximum stretch  $\lambda$  during the process segment a was fixed at 3.0. It was neither exceeded nor reduced in the later tests with the exception of the test conducted at 253 K. During the tests conducted at 253 K the specimens showed large stiffening effects. Since limitations due to failure of the bond between the steel flange and the vulcanized rubber were encountered, these tests were conducted by reducing the maximum stretch to 2.5. The corresponding Fig. for the test done at 253 K is not presented here for brevity.

The steps a and l applied in the segments *II, V, VIII, XI* of the temperature history were directed to investigate the effect of the temperature on the Mullins effect at three different maximum stretches. The steps b–k applied in the segments *II* and

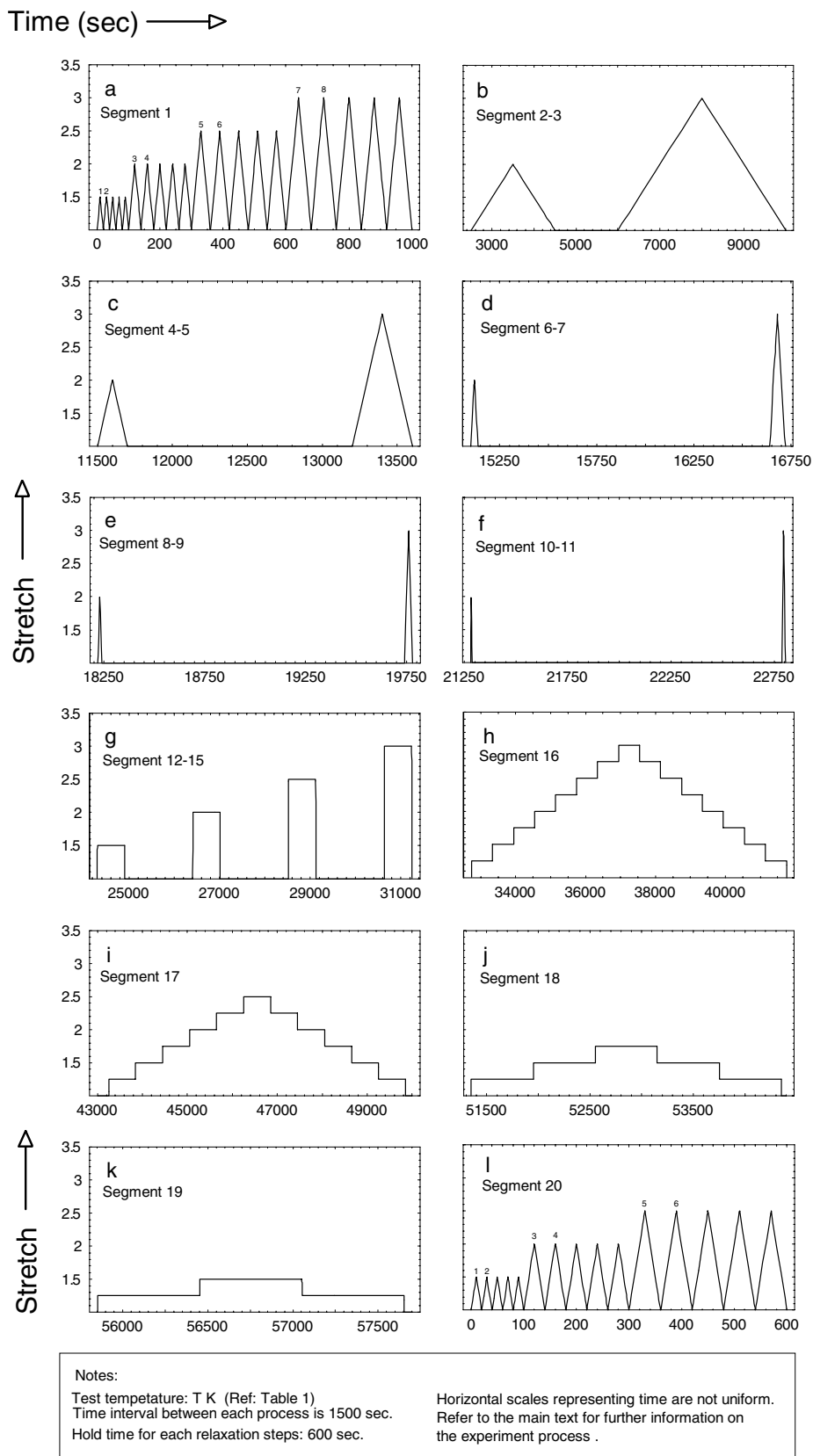


**Fig. 6** Sequence of applying deformation histories in specimens at different thermal equilibriums. The figure is to be read in conjunction with Fig. 5, Tables 1 and 2.

**Table 2** Details of deformation histories (Fig. 6) as applied on specimens.

Step A: Cyclic tests on virgin specimens with a view to observe and thereby to 'remove' the Mullins effect. Stretch was applied at a rate of 0.05/s at 263 K, 293 K, 313 K, and 333 K. In conducting the test at 253 K, the last five stretch cycles going up to 3.0 stretch were omitted.

Steps B–F: Cyclic tests are driven on specimens that had the history of A. The specimens were subjected to cyclic tension up to stretch levels of 2.0 and 3.0, respectively, for five different stretch rates (0.001/s, 0.01/s, 0.05/s, 0.1/s, 0.25/s) as shown in Fig. 5 at different temperatures of 263 K, 293 K, 313 K, and 333 K. In conducting the test at 253 K the stretch amplitudes were chosen to be 2.0 and 2.5.

Step G: Simple relaxation tests were driven on the specimen that had the stretch histories A–F. The maximum stretch levels for the simple relaxation tests were chosen to be 1.5, 2.0, 2.5, and 3.0 for 263 K, 293 K, 313 K, and 333 K. In conducting the tests at 253 K, the simple relaxation test at 3.0 stretch was omitted. The stretch rate during each loading and unloading phase was 0.25/s.

Step H–K: Three multi-step cyclic relaxation tests were driven at three different maximum stretch levels of 3.0, 2.5, and 1.75 at 263 K, 293 K, 313 K, and 333 K. To conduct the tests at 253 K, the corresponding maximum stretch amplitudes were at 2.5, 1.75, and 1.5. The stretch increment or decrement in each step was chosen to be 0.25 for each tests. The stretch rate during each loading and unloading phase was 0.25/s.

Note: The Table is to be read in conjunction with Figs. 5 and 6, and Table 1.

*XIV* of the temperature process were introduced to study the effect of heat treatment on the strain rate dependence, stress relaxation and hysteresis. Prior to the application of the strain history in segment *XIV*, all specimens were tempered at 363 K (segment *XII*) to allow healing of the softening effect due to segment *XI*. The tests (a–k) conducted between 263 K–333 K had the total duration of 59,153 seconds for each reference temperature ( $T$  K). The testing procedure (a–k) prescribed at 253 K has a shorter duration (57,740 second) since the applied stretch was lower.

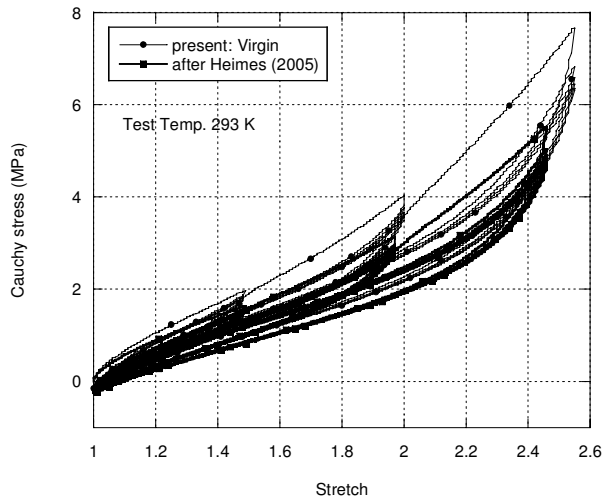
### 3 Results and discussion

In Sect. 1, the general thermo mechanical behaviour of filler-reinforced rubber and the influence of the temperature history were summarized. Furthermore, temperature- and deformation-induced crystallinity effects are presented. Both the available literature and the DSC data of the blend illustrate that the crystallites formed within the macromolecular network can disappear through melting processes at sufficiently high temperature levels. Sect. 1 has also presented the definition of the Mullins effect, the possibility of healing by exposing the material to elevated temperatures, and the effects of strain rate and stress relaxation. They form the background of the tests in Sect. 2 in order to obtain experimental information about the thermo rheological effects which occur due to temperature and deformation. We study the temperature dependence of the Mullins effect in specimens with crystallinity, the healing due to tempering, the reduction of crystallinity during tempering, and the Mullins effect in healed specimens with reduced crystallinity. Both the strain rate dependence and the stress relaxation at different temperatures as well as the effects due to heat treatment are investigated. The following sub-sections present the experimental results together with a discussion.

#### 3.1 Crystallization in the specimens on long term storage

In Fig. 7, the stress response of the virgin specimen at 293 K deformed with the stretch process (Fig. 6a) is compared with the response obtained by applying a similar deformation history on a newly vulcanized specimen [42]. The test reported in Heimes [42] was conducted in the same testing machine as the current one but at a bit higher speed of 0.10/s. Although, at a higher stretch rate a greater and stiffer stress response is expected, the response of the specimen stored over three years at room temperature is stiffer. This observation suggests that a certain part of the amorphous fraction of the specimen got gradually transformed to the crystalline phase during the long term storage at room temperature. A further comparison shows that the virgin specimen stored for three years showed stiffer responses under similar stretch levels during both loading and unloading. This effect is due to an increase in the crystallinity. Wood and Roth [15] observed similar effects in vulcanized NR aged for three months at 298 K (see also Wood and Bekkedahl [16], pp. 368–369). Such a crystallization-induced increase in stiffness is important from the viewpoint of obtaining an acceptable performance of rubber products over their service life.

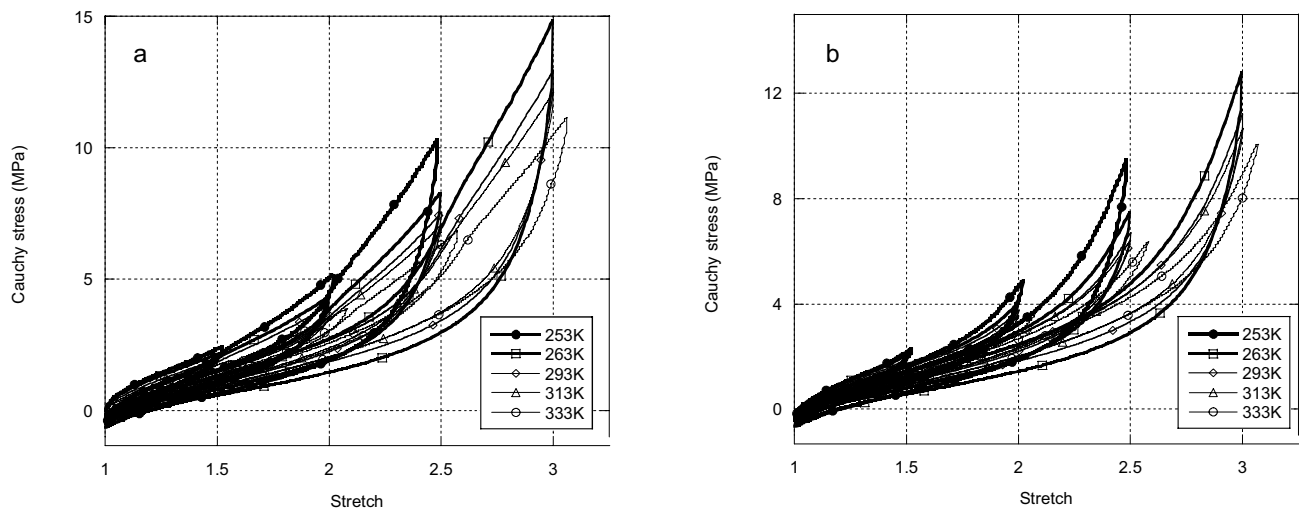
Thus, in further experimental studies, additional X-ray measurements are needed and should be provided in order to determine the degree of crystallinity corresponding to the different stretch and temperature histories.



**Fig. 7** Stress-stretch response of virgin specimen at room temperature (293 K). Response obtained from the virgin specimen at stretch rate 0.05/s in 2007 is compared with the response from the test conducted in 2004 on virgin specimen at 0.1/s, as documented in Heimes (2005).

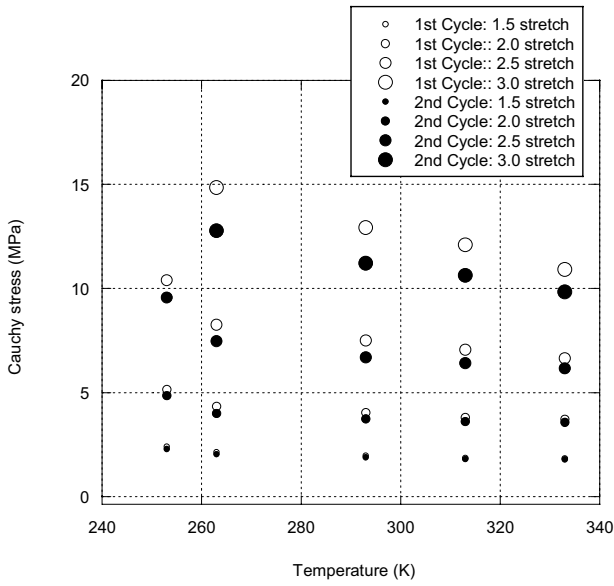
### 3.2 Temperature dependence of Mullins effect in crystallized specimen

Fig. 8a shows the effect of the specimen temperature on the first loading cycles (Cycle 1, 3, 5, 7; Fig. 6, Step a), while Fig. 8b shows the same effect observed in the second loading cycles (Cycle 2, 4, 6, 8; Fig. 6, Step a). The stress amplitudes recorded in the second loading cycles (Fig. 8b) are lesser than those in the first cycles (Fig. 8a). These reductions can be interpreted as the Mullins effect. However, it should be noted that a specimen at a lower temperature contains a larger crystallinity and a lower amorphicity. In addition, it should have a lower molecular mobility and a larger rate dependence. By taking these points as background, we note that the energy absorption, represented by the areas of the stress-stretch curves of a cycle, is much larger at low temperatures and it decreases with the increase of temperature.



**Fig. 8** Mullins effect characterized by stretch amplitude dependent softening phenomena at different temperatures. All observations are made 0.05/s stretch rate as per the experimental scheme shown in Fig. 6, Step a. (a) The first cycles (1, 3, 5, and 7); (b) The second cycles (2, 4, 6, and 8).

In Fig. 9, the maximum stresses recorded in cycles 1, 3, 5, 7 (Fig. 6, Step a) are compared with those belonging to the cycles 2, 4, 6, 8 (Fig. 6, Step a) and are plotted as a function of temperature ( $T$  K). The plot shows that the softening increases with increasing stretch amplitude and decreasing temperature. A change is observed at temperature levels below 263 K: in comparison with the softening observed at 253 K, the softening is quite small at 333 K. The stress responses of virgin specimens recorded in the tests at 263 K are presented in Fig. 10 as functions of time. A diminishing trend of the softening at each stretch amplitude is noted after the second cycles (cycles 2, 4, 6, 8). In addition, the peaks of the stress response clearly depict the deformation dependence of the Mullins effect: the higher the applied stretch the higher is the softening effect. At the end of each cycle, the applied stretch was set to zero (Fig. 6, Step a). This causes that the stress changes its sign due to viscosity induced strain rate effects. The stress responses belonging to the other temperatures lead



**Fig. 9** Stress amplitudes at first cycles (1, 3, 5, and 7) and second cycles (2, 4, 6, and 8) plotted as a function of temperature. Mullins softening effect is viewed as the difference in stress amplitude over the first and second cycle. The results are from the *virgin specimens* that have shown to have developed significant crystallinity during their shelf life (Fig. 7).

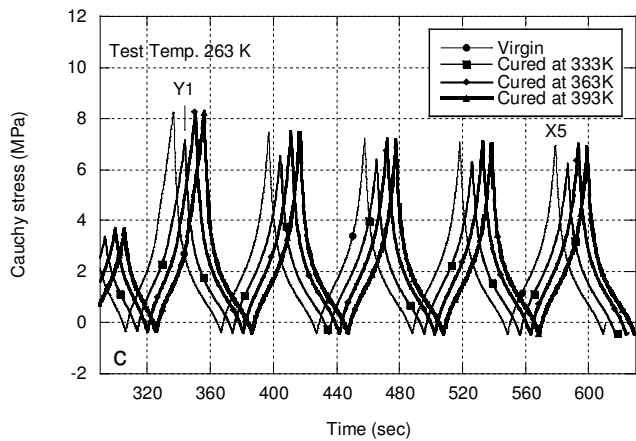
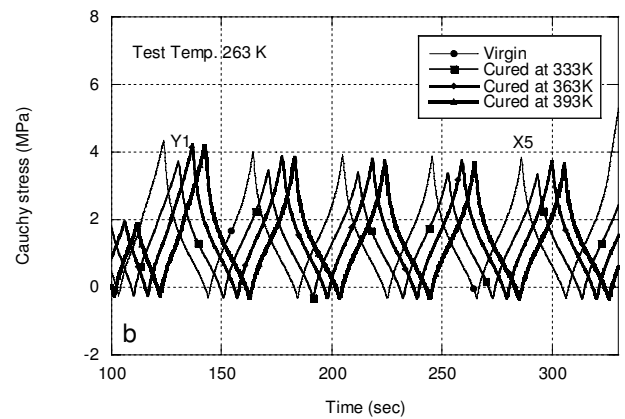
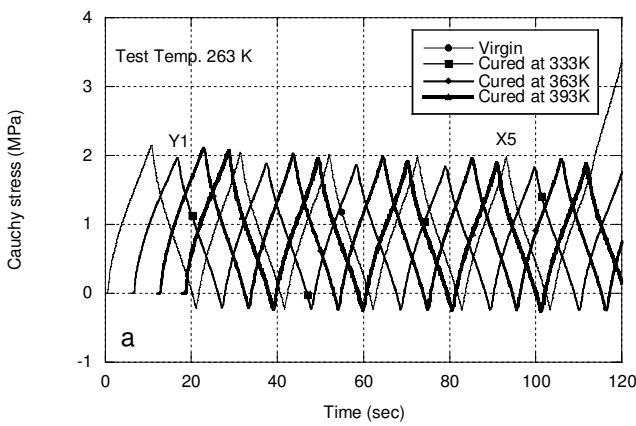


**Fig. 10** Stress histories obtained from virgin specimen and specimens tempered at different temperatures. The mechanical processes (Fig. 6 and 6a) were applied at 263 K in each of the tests. For the purpose of understandable illustration, the stress histories have been separated from each other by 6 s. In reporting the stress history for virgin specimen, records only up to first 600 seconds are plotted.

to the same conclusions and are skipped for brevity. These observations (Fig. 10) are consistent with the earlier work at room temperature (Lion [11]).

### 3.3 Effect of heat treatment temperature on the healing behaviour

The consequences of successive temperature increases during the heat treatment (from 333 K to 393 K; Fig. 5, Steps III, VI, IX) on the healing behaviour of the Mullins effect are presented in Figs. 10a, 10b, and 10c. They show different segments of the stress responses corresponding to the different stretch amplitudes. The parameter in these tests is the temperature

during the heat treatment which was 24 hours in duration. In performing the mechanical tests, the specimen temperature was held constant at 263 K and the stretch rate was set to 0.05/s. Due to the same stretch rate in all tests, strain rate effects are not considered. The virgin specimen was deformed with the stretch history as shown in Fig. 6 (Step a) and the tempered specimen with the stretch history shown in Fig. 6, Step I. During the first 600 seconds both histories are equal. The stretch history in Fig. 6, Step I is shorter in duration due to the omission of the last five cycles going up to a stretch of 3.0. In order to point out the relevant effects in Fig. 10, the stress histories of the tempered specimens have been shifted by 6, 12, and 18 seconds relative to the response of the virgin specimen.

The comparison of the stress peaks of the virgin specimen at 263 K and that tempered at 333 K (Fig. 5, Segment III) and tested at 263 K shows an interesting trend: even the fifth peak (marked X5) of the virgin specimen lies at a higher value than the first peak (Y1) produced by the specimen after tempering at 333 K (Fig. 5, Segment III). This amplitude reduction is the result of the application of the deformation process (Fig. 6b-k, Fig. 5-Segment II) which the specimen observed before experiencing the heat treatment (Gentot et al. [27]). The effect of the temperature treatment at 333 K is small. But after tempering the specimen at 363 K for 24 hours, the stress peaks become comparable to those of the virgin specimen. The heat treatment at a higher temperature facilitates molecular motions and increases the rate of reconstruction of ruptured bonds between the filler aggregates and the rubber molecules. However, from the current measurements it is not clear whether the bonds reconstructed upon applying temperature are physical or chemical in nature. The experimental data and its interpretation obtained from mechanical tests call for the necessity of measuring the amount of heat which is absorbed or dissipated by the specimens during the heat treatment. Precise measurement of the heat exchange in a DSC device provides more information in this context. After the heat treatment, the specimen was cooled down to room temperature and then to 263 K for performing the mechanical tests. During this cooling process, it is possible to completely or partially regenerate the crystalline structure. Finally, the stress-stretch responses of the virgin specimen and those of the specimen tempered at 363 K for 24 hours are compared (Segments II and VIII, Fig. 5) in Fig. 11: the match is nearly perfect.

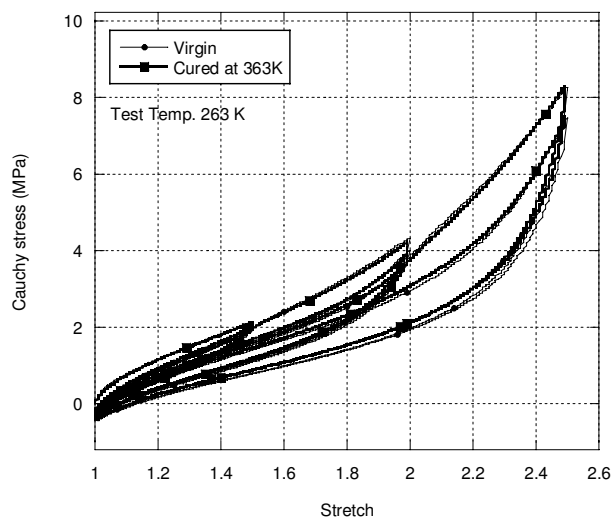


**Fig. 11** Comparison between the stress-stretch response from virgin specimen and that from the specimen after tempering at 363 K (Fig. 5, Segment VI).

A tempering of the specimen at a higher level of 393 K (Fig. 5, Segment IX and Fig. 10) was not found to cause an appreciable increase in the stress amplitude. This observation also demonstrates the existence of a threshold temperature for attaining the virgin material behaviour through thermally-activated healing processes. The comparison of the stress responses obtained after tempering the specimen at 333 K, 363 K, and 393 K does not suggest any stretch history effect,  $l$ , (Fig. 6). The significant role of the temperature on the appearance of healing within a specific time interval can thus be recognized.

### 3.4 Melting of crystalline structure and transformation of crystalline fraction to amorphous fraction by thermal ageing

In Fig. 12, the isothermal stress-stretch responses of the virgin specimens (Step a, Fig. 6) at temperature levels of 253 K, 293 K, and 333 K are compared with those of the specimens after tempering at 393 K (Fig. 5, Segment XI). More or less pronounced differences in the responses between the virgin and the heat-treated specimens are observed. Comparing Figs. 12a, 12b, and 12c, the responses between the virgin and the tempered specimen are found closer at 253 K, while at 293 K and 333 K the differences get wider. In general, the tempered specimens show a softer behaviour during the loading phase. Furthermore, at 293 K and 333 K a softer response during the unloading phase is noted. All these observations are in contrast with those reported in Fig. 11 at 263 K, where a perfect match is observed. This peculiarity between the

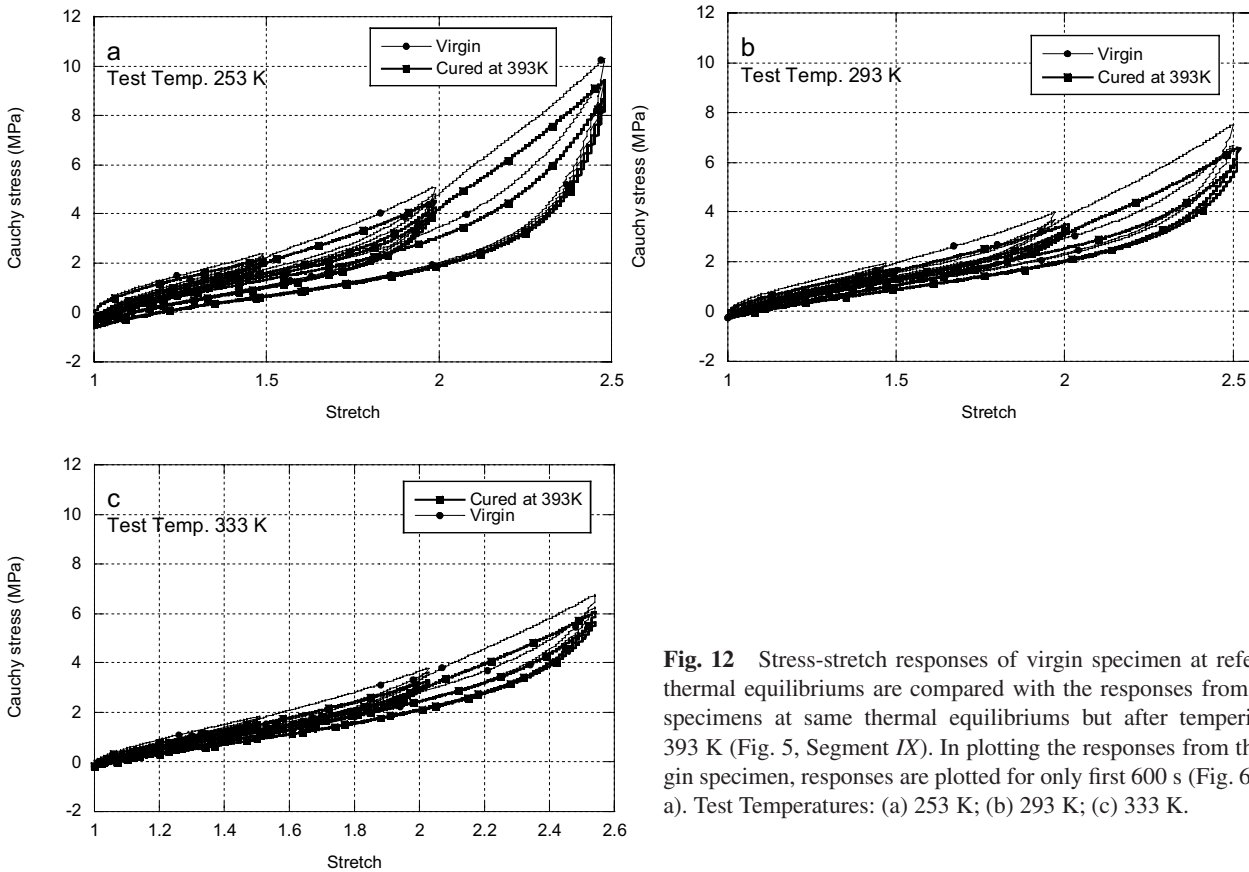


**Fig. 12** Stress-stretch responses of virgin specimen at reference thermal equilibria are compared with the responses from same specimens at same thermal equilibria but after tempering at 393 K (Fig. 5, Segment IX). In plotting the responses from the virgin specimen, responses are plotted for only first 600 s (Fig. 6, Step a). Test Temperatures: (a) 253 K; (b) 293 K; (c) 333 K.

responses presented in Figs. 11 and 12 has its explanation in the changing degree of crystallinity. A certain degree of crystallinity existing in the virgin specimen (Fig. 7), is reduced by the heat treatment (Fig. 5, Segments III, VI, IX) and restored by conditioning at a temperature below 273 K for a few hours before performing the mechanical test (Fig. 5, Step XI and Fig. 6, Step 1). In obtaining these responses, the durations for which the specimens were exposed to the temperature (including their path of cooling or heating from the room temperature) were the same. The stretch and heating rates were also the same. In this context, the temperature dependence of the crystallization rate needs to be taken into account. It is higher below 273 K, passes through a maximum at around 260 K–280 K (Fig. 4a) and diminishes rapidly with increasing temperature or by approaching the glass transition temperature  $T_g$  due to the reduced mobility of the macromolecules (see Wood and Roth [15]; Wood and Bekkedahl [16]; Luch and Yeh [77]; Stevenson [18]; and Sect. 1.3.2). Nevertheless, the temperature at which the maximum crystallization rate occurs depends on a number of variables including the vulcanization procedure, the type of rubber and its composition. In the present work, the authors assume that the rate of crystallization of their NR/BR blend is maximal in the neighbourhood of about 263 K (see Fig. 4a for an independent confirmation via DSC tests). This may be the major reason behind obtaining the perfect match between the stress responses of the virgin specimens and those of the tempered (363 K) specimens at 263 K. In the other temperature ranges, the match between the virgin and the tempered specimen is inferior. To determine the temperature value which is most convenient for crystallization, the exo- and endothermal heat exchange behaviour of semi-crystalline rubber specimen should be studied in detail with the DSC technique. Performing such tests in parallel to the mechanical tests may help establishing further correlations between the measurements. In addition to this, the degree of crystallinity should be quantified with X-ray measurements.

To justify the reduction of the crystallinity of the specimens during the heat treatment (Fig. 5, Segments III, VI, IX), a test reported by Heimes [42] is considered. It is compared with the current stress response obtained at 293 K from the specimen after tempering for 24 hours at 393 K via Segment XI of Fig. 5 (also see Fig. 12b). The comparison is presented in Fig. 13, where a good conformity is noticed. During the loading paths, there are weak differences between the current measurement and that of Heimes. When the small difference in the stretch rates is considered, an excellent correlation between the tests driven in 2004 and 2007 can be recognized. We conclude that the crystalline fraction of the specimen which is transformed from the amorphous to the crystalline phase during the long term storage of about 3 years was retransformed again to the amorphous phase upon tempering. This observation justifies the idea of storing the specimen at an elevated temperature before driving the actual tests. Then, the existing crystals melt and the effects resulting from crystallinity are removed

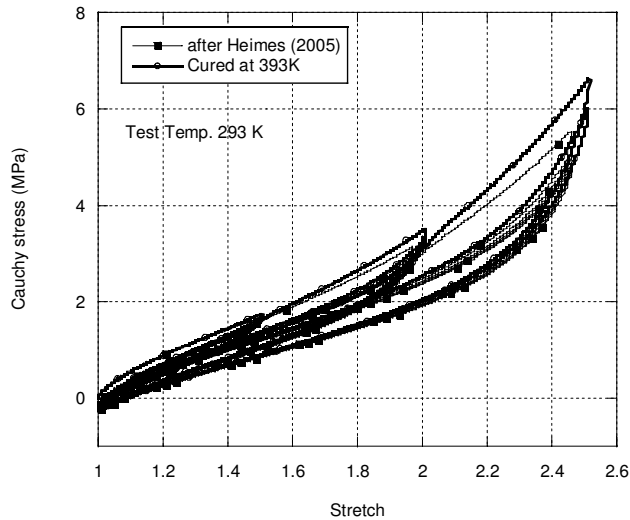


**Fig. 13** Stress-stretch response from specimen tempered at 393 K (Fig. 5, Segment IX) and tested at room temperature (293 K) is compared with the measurements of Heimes (2005) made also at room temperature. To obtain response from the tempered specimen, deformation process (Fig. 5) was applied at stretch rate 0.05/s in 2007 whereas Heimes [42] applied a similar deformation process but at 0.1/s stretch rate in 2004.

(Fuller et al. [20]). Furthermore, our test data show that the tempering process does not bring any irreversible character in the stress-strain behaviour. But it underlines the necessity of considering the whole temperature history in measuring and understanding the current mechanical behaviour of rubber.

### 3.5 Temperature dependence of Mullins effect in specimen having reduced crystalline fraction due to melting

The transformation of the crystalline fraction of the material to the amorphous phase due to heat treatment has been resolved in the last subsection together with the illustrations in Figs. 12 and 13. Now, we discuss the temperature dependence of the Mullins effect after tempering, i.e. when the material contains a reduced crystallinity. Fig. 14 presents the stress softening due to the Mullins effect (Fig. 1c) as a function of temperature. The softening effect of the virgin specimens is compared with that of the specimens tempered at 363 K and 393 K. The comparison shows that at temperatures of and above 293 K, the virgin specimens show a more pronounced softening than the tempered ones. This difference diminishes when the reference test temperature is increased from 293 K and approaches towards 363 K. In contrast, at reference test temperatures below 273 K, a weak difference in the Mullins effect is noted between the virgin and the tempered specimen. The duration of the test with the virgin specimens above 293 K was not long enough in order to melt the crystalline structure completely which is built up during the long term storage. In contrast, the long tempering process in the heat chamber (for 24 h in each step, Fig. 5) was much longer in duration and finally led to a significant reduction in the crystallinity. This indicates that

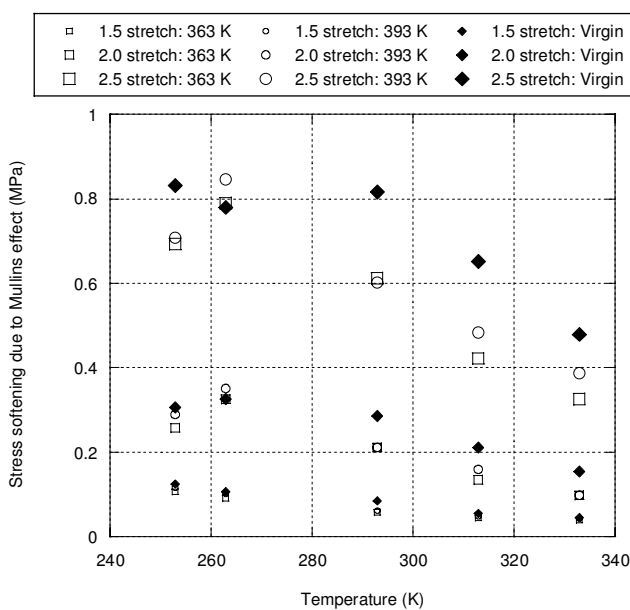


**Fig. 14** Mullins softening effect is viewed as the difference in stress amplitude over the first and second cycle (stress softening effect). Stress amplitudes at first cycles (1, 3, 5, and 7) are deducted from those recorded at second cycles (2, 4, 6, and 8) and plotted as a function of temperature. The results from the virgin specimens (at  $T$  K) that have shown to have developed significant crystallinity during their shelf life (Fig. 7) are compared with those after tempering at 363 K and 393 K (Figs. 5 and 6).

the physico-chemical states which are responsible for the Mullins effect may lie in both the amorphous and the crystalline regions of the network. Those regions of the amorphous phase that contain the filler particles are hardly converted to crystalline parts (Poompradub et al. [80]). On the contrary, the crystallinity is more related to the molecular network of the rubber chains: a deformation or temperature induced transformation between the amorphous and crystalline fractions of the chains of the rubber network is therefore more readily possible. In addition to other known findings (Bueche [107, 108]; Wood and Bekkedahl [16]), the role of the fillers on the Mullins effect and the effect of vulcanization on the rate of crystallization, the current observations also fit well with the earlier observations (Sogolova [109]).

### 3.6 Strain rate dependence in virgin specimens and effect of tempering

Figs. 15–18 present the effect of the strain rate on the cyclic material behaviour of the NR/BR blend between 253 K and 333 K in both virgin specimens (Segment II of temperature history, Fig. 5) and tempered specimens (Segment XIV of temperature history, Fig. 5). We present the results of cyclic tension tests conducted between stretch levels of 2.5 and 3.0. The tests conducted with stretch levels below 2.5 are omitted for brevity. The equilibrium stress-stretch curves are obtained from multi-step relaxation tests and are plotted to illustrate the rate dependent phenomena under isothermal conditions. The rate dependence is more pronounced at lower temperatures, but at higher temperatures the specimens show softer responses. The specimens tested at higher temperatures display in general a less pronounced hysteresis. Yet, the results obtained at

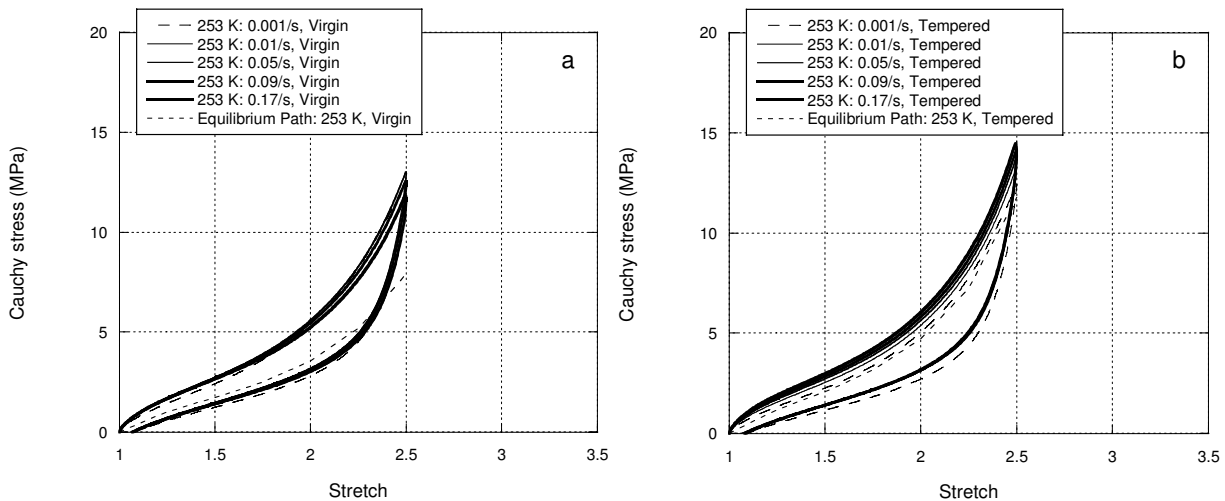


**Fig. 15** Effect of strain rate on stress-strain responses in virgin specimens and tempered specimens. Tests are conducted at 253 K.

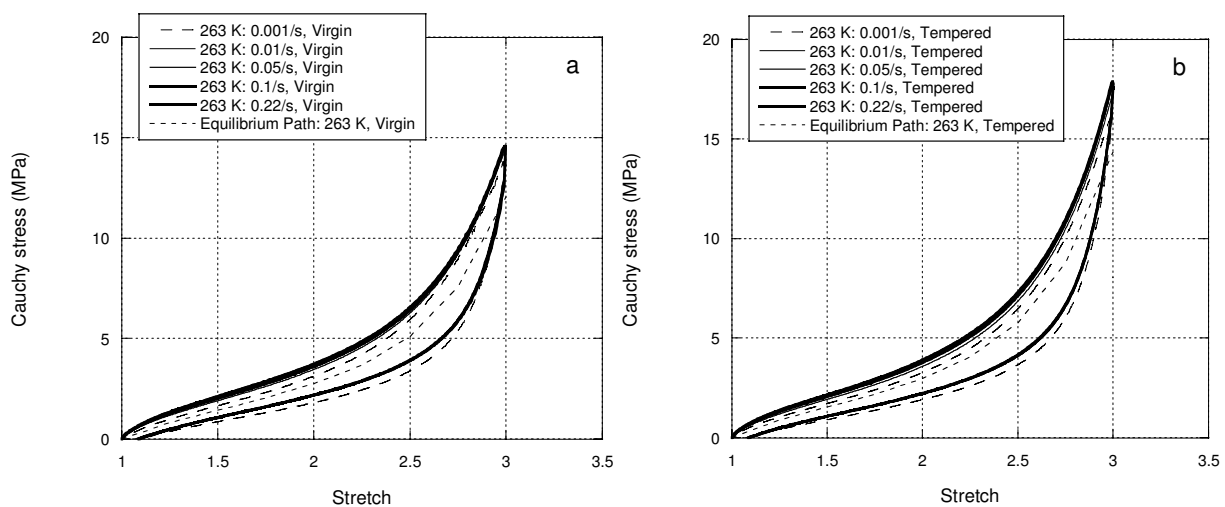


**Fig. 16** Effect of strain rate on stress-strain responses in (a) virgin specimens and (b) tempered specimens. Tests are conducted at 263 K.

253 K and 263 K in the virgin and the tempered specimens (Figs. 15–16) have some striking features in the loading part. The stress responses of the virgin specimen (Fig. 15a, Fig. 16a) at different strain rates seem to merge to each other. More particularly, the stress response obtained at 253 K (Fig. 15a) with a strain rate of 0.001/s is found to be stiffer than that measured with a rate of 0.17/s, when the stretch level crosses 1.75. Such an increase in the stiffness at a slower rate was also observed at 263 K (Fig. 16a), but at a higher stretch level ( $\lambda_1 = 3.0$ ). This peculiarity in the stress-strain behaviour is caused by the following fact: at a slow strain rate of only 0.001/s the virgin specimen is exposed for a fairly long time at a low temperature and a large deformation. This allows an additional crystallization to take place which is further clarified, when the results shown in Fig. 15a obtained at 253 K are compared with those shown in Figs. 17a (at 293 K) and 18a (at 333 K): the rate dependence is more pronounced in the virgin specimens when the test temperature is higher and the crystallinity smaller. Yet, all specimens show more pronounced rate effects after experiencing a temperature history up to 393 K (Figs. 15b, 16b, 17b, 18b).

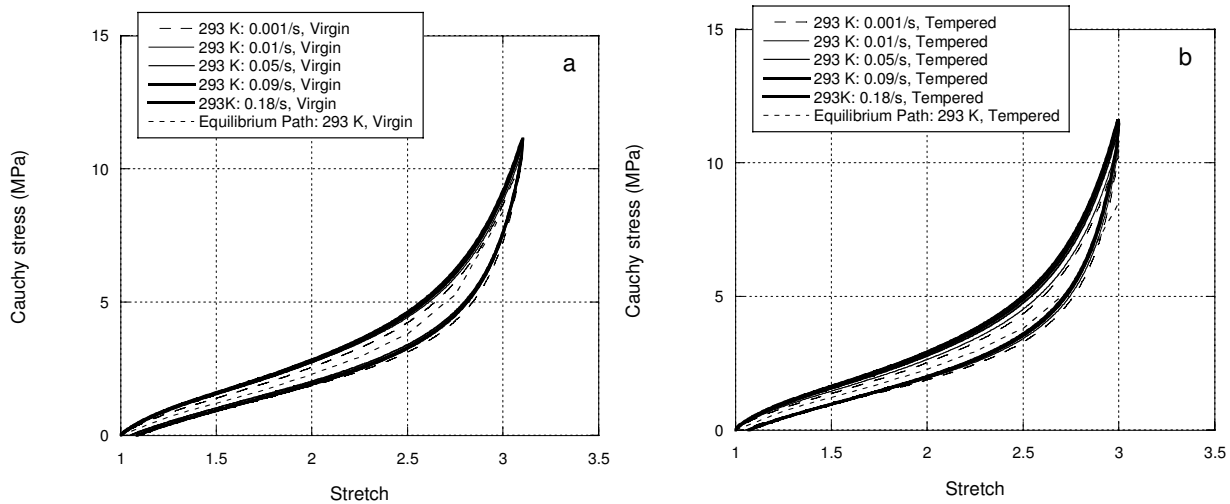


**Fig. 17** Effect of strain rate on stress-strain responses in (a) virgin specimens and (b) tempered specimens. Tests are conducted at 293 K.

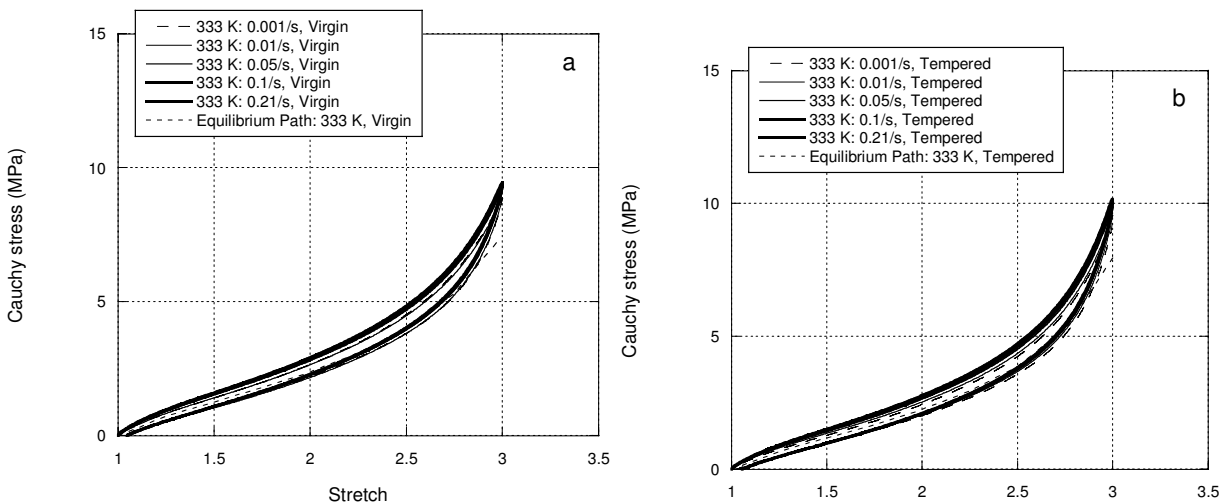


**Fig. 18** Effect of strain rate on stress-strain responses in (a) virgin specimens and (b) tempered specimens. Tests are conducted at 333 K.

### 3.7 Stress relaxation phenomena in virgin specimens and effect of tempering

Simple relaxation tests were conducted with both virgin and tempered specimens at different strain levels to study the deformation dependence of the stress relaxation. Figs. 19 and 20 summarize the recorded stress histories. The amounts

of the stress relaxation are indicated by the differences of the stress levels between the beginning and the end of the test (see also Fig. 3). They are found to be more pronounced under higher strains. This observation conforms to the previous results of NR and HDR (Amin et al. [8, 38]) under shear deformations and compression. All specimens show a longer stress relaxation with decreasing temperature.

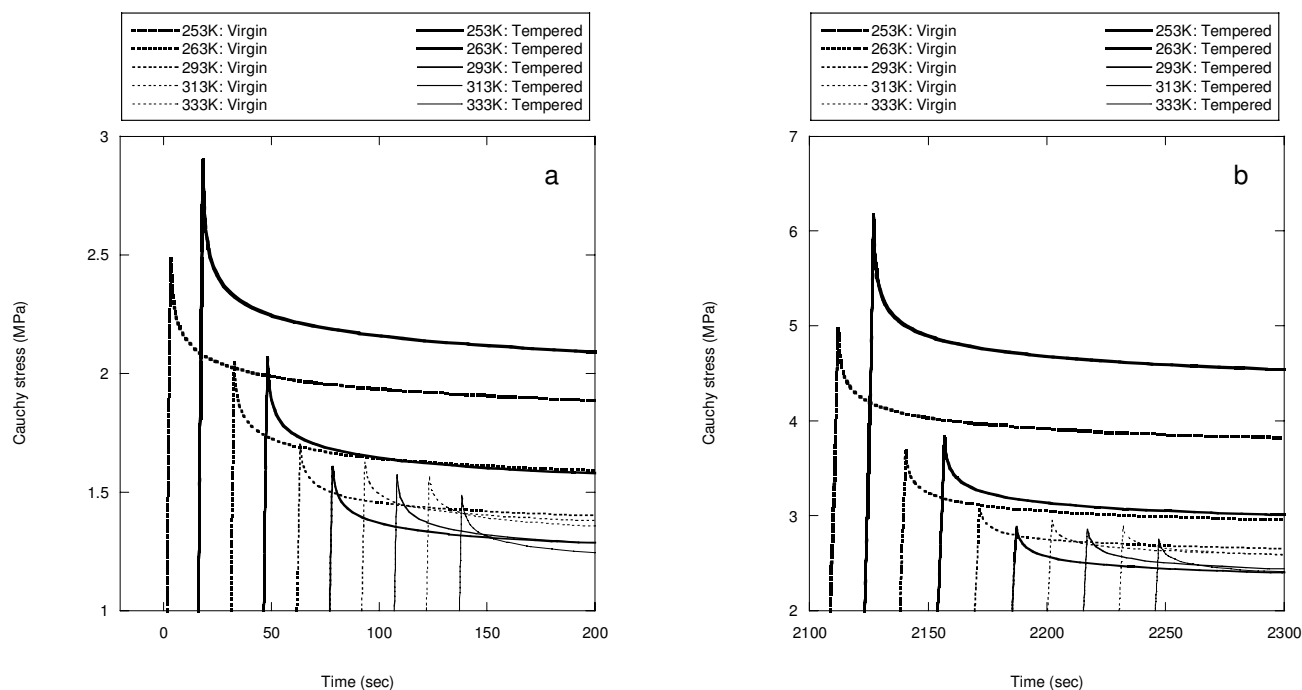


**Fig. 19** Stress relaxation histories obtained from simple relaxation tests on virgin specimens and tempered specimens at lower stretch levels. (a)  $\lambda_1 = 1.5$ ; (b)  $\lambda_1 = 2.0$ .

The equilibrium stress-strain relation is the stress response of the material belonging to infinitely slow deformation processes or to relaxation processes with hold times of infinitely long duration. These relations can be measured with multi-step relaxation tests if the termination points of the relaxation processes are connected in a stress-strain diagram. It should be noted that the durations of the hold times must be long enough such that all time-dependent internal processes occurring in the material are decayed. At temperature levels higher than 263 K, we observe a unique equilibrium curve which is independent on temperature (Fig. 21). But at the lower temperature levels of 253 K and 263 K, the curves show a stiffer behaviour. This behaviour finds its physical interpretation by taking the simple relaxation tests plotted in Figs. 19 and 20 into account. They show an essentially longer relaxation behaviour of the tested NR/BR blend at smaller temperatures. Since the hold times of 1500 s duration were the same in all relaxation experiments, the equilibrium states are not reached in the low temperature multi-step relaxation tests. The tempered specimens have shown the same effect in a more pronounced way.

The instantaneous stress response of a material is the stress-strain relation which corresponds to infinitely high deformation rates. It can be experimentally determined, if the deformation rate is sufficiently high such that no decay of the internal time-dependent processes can occur. Since the maximum strain rates which are realizable with our testing machine are between 0.17/s and 0.22/s we denote the measured responses as quasi-instantaneous responses. The quasi-instantaneous responses at 253 K and 263 K, 313 K, 333 K are compared for the virgin and the tempered specimens in Fig. 22. The results suggest a diminishing effect of the temperature on the quasi-instantaneous stress response at high temperature levels. At low temperature, the opposite effect is clearly observed. At higher temperature levels the relaxation times of the blend become essentially smaller such that the strain rates of about 0.2/s are too small to avoid any kind of internal decay behaviour.

After tempering, the quasi-instantaneous and the equilibrium stresses obtained from the tempered specimens in simple relaxation tests at a temperature below 263 K were recorded. They are larger than those obtained from the virgin specimens (Figs. 19, 20). Above 263 K, the trend was found to move in the opposite direction.

Finally, we look once again at the applied deformation history (Fig. 6) at a particular temperature (Table 1) to compare the rate-dependence through two sets of different tests: cyclic tension tests (Figs. 15-18, 22) and relaxation tests (Figs. 19-21). We note that the conditioning time (ASTM D 832-92 [100]) denoted by the duration that a specimen has passed in the temperature chamber before performing the respective tests was much shorter in the cyclic tension tests than in the

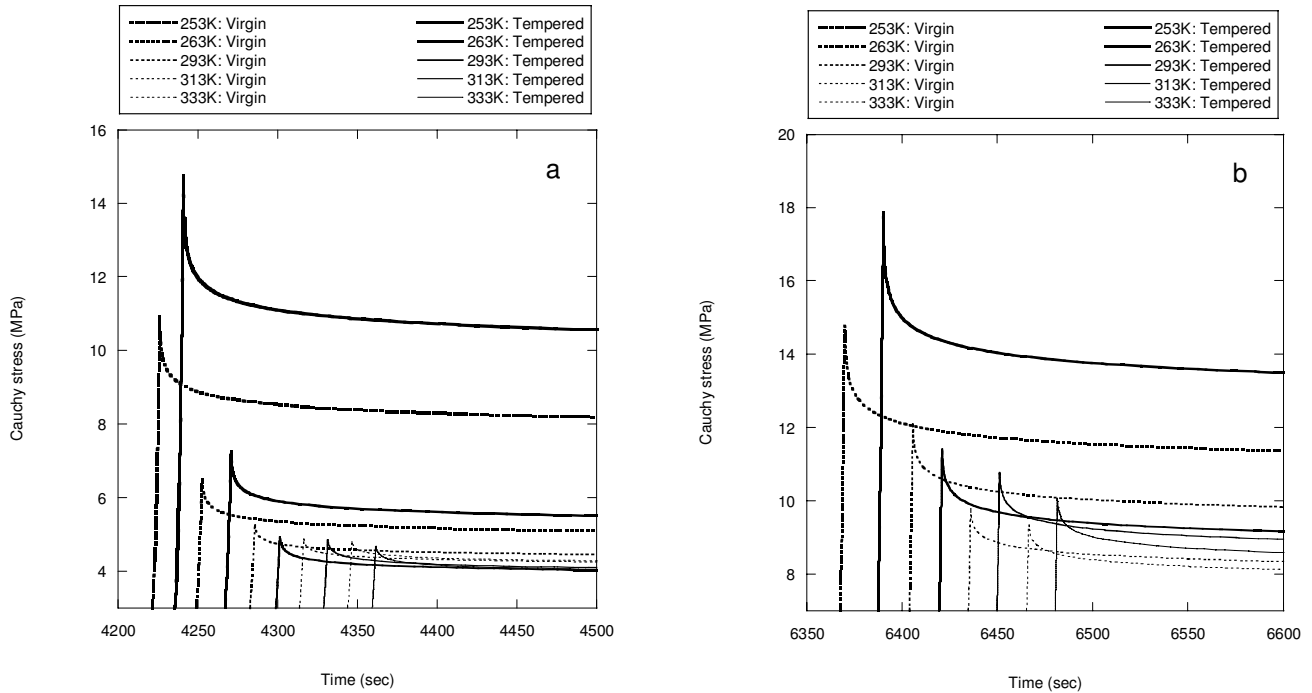


**Fig. 20** Stress relaxation histories obtained from simple relaxation tests on virgin specimens and tempered specimens at larger stretch levels. (a)  $\lambda_1 = 2.5$ ; (b)  $\lambda_1 = 3.0$ .

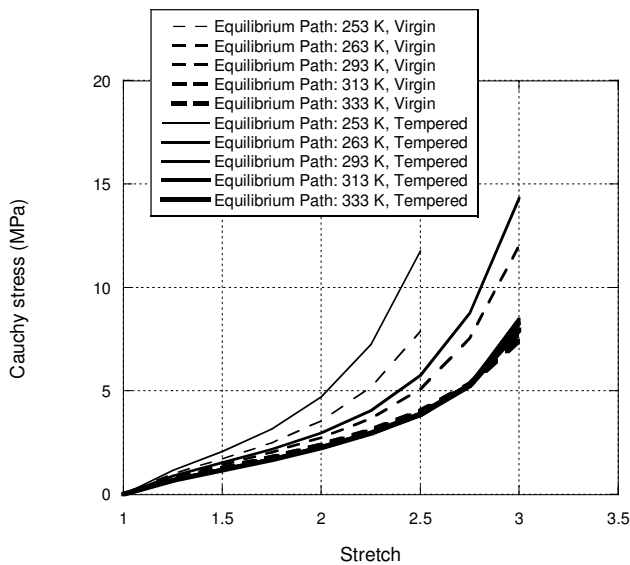


**Fig. 21** Equilibrium responses traced from multi-step relaxation tests on virgin specimens and tempered specimens at different thermal equilibria.

relaxation tests. Considering both a temperature-dependent induction time and an equilibrium state for the crystallization (Stevenson [18]), the quantitative measurements of the degree of crystallinity via X-ray measurements at every stage of the test sequence give more information about the variation between the two sets of test results.

### 4 Conclusions

A comparison between a large number of experimentally-observed stress-stretch curves conducted on both newly vulcanized rubber and specimen vulcanized in the same batch but stored for three years at room temperature suggests stiffening effects to take place with time due to crystallization. Applying an adequate heat treatment it is possible to reduce the crystallinity which has been developed within the molecular structure of the rubber with time. Experimental results further

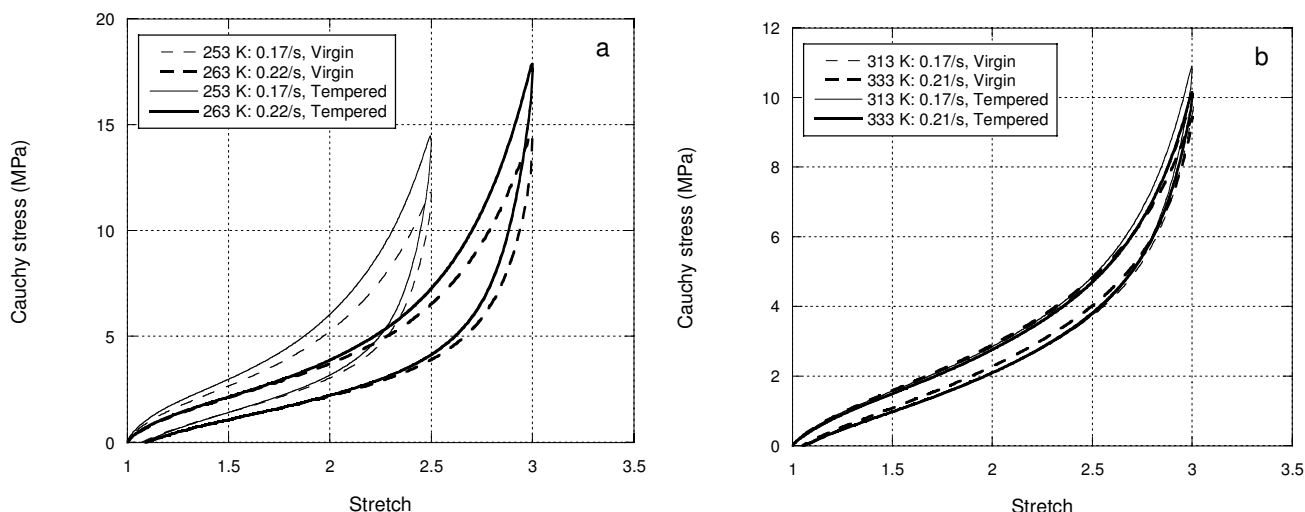


**Fig. 22** Instantaneous responses obtained from cyclic tension tests at high strain rates at different thermal equilibria on virgin specimens and tempered specimens. (a) 253 K and 263 K; (b) 313 K and 333 K.

indicate that a decrease in the specimen temperature leads to more pronounced hysteresis properties together with an increased softening effect. This observation is rather general in nature and has a relation to the amount of crystallinity in the material. Tempering of the softened specimens leads to healing such that the Mullins effect can be observed once again. A comparison of the results obtained from the virgin and the tempered specimens tested at different temperatures suggests that the temperature dependence of the melting and recrystallization rates play a role on the Mullins effect in the virgin and the healed specimens. However, the tempering of the specimens at elevated temperatures for a specific time showed the existence of a threshold temperature which is necessary to completely heal the specimens. Yet, all these observations are coupled with the strain rate dependence of the material. In our experiments, we also observe that the degree of crystallinity influences both the equilibrium and the quasi-instantaneous stress responses. But its influence on the viscous or rate-dependent material behaviour seems to be comparatively weak.

From our point of view, the experimental data provided in this essay appears to be useful for the future development of physically-based thermo mechanical material models for filler-reinforced rubber. We have seen that the material behaviour of the NR/BR rubber blend does not depend only on the deformation history and the current thermodynamic temperature, but also on the entire temperature history. In addition, healing does occur. It is a challenge for the future to develop physically-based and thermo mechanically-consistent theories representing the material behaviour of rubber as a functional of two variables, namely the deformation history and the temperature history. In addition to the pure investigation of the mechanical stress responses, the thermal response functions like the internal or the free energy or the entropy have to be investigated [110]. To this end, not only testing the stress-stretch behaviour as it is common practice in engineering but also additional experimental techniques like DSC, TMA, or TGA are absolutely required.

**Acknowledgements** Dr. A.F.M.S. Amin is grateful to the Alexander von Humboldt foundation for granting a Georg Forster fellowship that enabled him to stay at the Institute of Mechanics at the Faculty of Aerospace Engineering in the University of the Federal Armed Forces Munich during February 2007 until July 2007 to conduct this Joint Collaborative Research. Special thanks also go to the Bangladesh University of Engineering and Technology for granting Dr. Amin a leave facility for the stay. The authors are also much grateful to Dr. Thomas Heimes for providing the digital version of his measurements that was reported in his doctoral dissertation.

## References

- [1] H. Morawetz, History of rubber research, *Rubber Chem. Technol.* **73**, 405–426 (2000).
- [2] J. M. Kelly, *Earthquake Resistant Design with Rubber* (Springer-Verlag, London, 1997).
- [3] C. M. Roland, Naval applications of elastomers, *Rubber Chem. Technol.* **77**, 542–551 (2004).
- [4] P. Haupt, *Continuum Mechanics and Theory of Materials* (Springer-Verlag, Berlin, 2000).
- [5] P. Blümler and B. Blümich, NMR imaging of elastomers: a review, *Rubber Chem. Technol.* **70**, 468–518 (1997).
- [6] J. S. Bergström and M. C. Boyce, Mechanical behaviour of particle-filled elastomers, *Rubber Chem. Technol.* **72**, 633–656 (1999).
- [7] J. S. Bergström and M. C. Boyce, Large strain time-dependent behaviour of filled elastomers, *Mech. Mater.* **32**, 627–644 (2000).

- [8] A. F. M. S. Amin, M. S. Alam, and Y. Okui, An improved hyperelasticity relation in modelling viscoelasticity response of natural and high damping rubbers in compression: experiments, parameter identification and numerical verification, *Mech. Mater.* **34**, 75–95 (2002).
- [9] A. F. M. S. Amin, M. S. Alam, and Y. Okui, Measurement of lateral deformation of natural and high damping rubbers in large deformation uniaxial tests, *J. Test Eval., ASTM* **31**, 524–532 (2003).
- [10] L. R. G. Treloar, The elasticity and related properties of rubbers, *Rep. Prog. Phys.* **36**, 755–826 (1973).
- [11] A. Lion, A constitutive model for carbon black filled rubber: Experimental investigations and mathematical representation, *Contin. Mech. Thermodyn.* **8**, 153–169 (1996).
- [12] A. Lion, A physically based method to represent the thermo-mechanical behaviour of elastomers, *Acta Mech.* **123**, 1–25 (1997).
- [13] A. Lion, On the large deformation behaviour of reinforced rubber at different temperatures, *J. Mech. Phys. Solids* **45**, 1805–1834 (1997).
- [14] F. Bueche, Mullins effect and rubber-filler interaction, *J. Appl. Polym. Sci.* **5**, 271–281 (1961).
- [15] L. A. Wood and F. L. Roth, Stress-temperature relations in a pure gum vulcanizate of natural rubber, *J. Appl. Phys.* **15**, 781–789 (1944).
- [16] L. A. Wood and N. Bekkedahl, Crystallization of unvulcanized rubber at different temperatures, *J. Appl. Phys.* **17**, 362–375 (1946).
- [17] A. N. Gent, Crystallization and the relaxation of stress in stretched natural rubber vulcanizates, *Trans. Faraday Soc.* **50**, 521–533 (1954).
- [18] A. Stevenson, The influence of low-temperature crystallization on the tensile elastic modulus of natural rubber, *J. Polym. Sci.* **21**, 553–572 (1983).
- [19] A. N. Gent and L. Q. Zhang, Strain induced crystallization and strength of elastomers. I. cis-1,4-Polybutadiene, *J. Polym. Sci. B, Polym. Phys.* **39**, 811–817 (2001).
- [20] K. N. G. Fuller, J. Gough, and A. G. Thomas, The effect of low temperature crystallization on the mechanical behaviour of rubber, *J. Polym. Sci. B, Polym. Phys.* **42**, 2181–2190 (2004).
- [21] L. Mullins, Effect of stretching on properties of rubber, *J. Rubber Res.* **16**, 275–289 (1947).
- [22] L. Mullins, Thixotropic behaviour of carbon black in rubber, *J. Phys. Colloid Chem.* **54**, 239–251 (1950).
- [23] L. Mullins, Determination of degree of crosslinking in natural rubber vulcanizates. Part I., *J. Polym. Sci.* **19**, 225–236 (1956).
- [24] L. Mullins, Determination of degree of crosslinking in natural rubber vulcanizates. Part III., *J. Appl. Polym. Sci.* **2**, 1–7 (1959).
- [25] L. Mullins, Softening of rubber by deformation, *Rubber Chem. Technol.* **42**, 339–362 (1969).
- [26] L. Mullins, Engineering with rubber, *Chem. Tech.* **87**, 720–727 (1987).
- [27] L. Gentot, M. Brieu, and G. Mesmacque, Modelling of stress-softening for elastomeric materials, *Rubber Chem. Technol.* **77**, 759–775 (2004).
- [28] S. Krishnaswamy and M. F. Beatty, The Mullins effect in compressible solids, *Int. J. Eng. Sci.* **38**, 1397–1414 (2000).
- [29] G. Franceschinia, D. Bigonia, P. Regitnigb, and G. A. Holzapfel, Brain tissue deforms similarly to filled elastomers and follows consolidation theory, *J. Mech. Phys. Solids* **54**, 2592–2620 (2006).
- [30] M. F. Beatty and S. Krishnaswamy, A theory of stress-softening in incompressible isotropic materials, *J. Mech. Phys. Solids* **48**, 1931–1965 (2000).
- [31] L. R. G. Treloar, Stress-strain data for vulcanized rubber under various types of deformations, *Trans. Faraday Soc.* **40**, 59–70 (1944).
- [32] H. W. Greensmith, Rupture of rubber. VIII. Comparisons of tear and tensile rupture measurements, *J. Appl. Polym. Sci.* **3**, 183–193 (1960).
- [33] A. N. Gent, Relaxation processes in vulcanized rubber. I. Relation among stress relaxation, creep, recovery, and hysteresis, *J. Appl. Polym. Sci.* **6**, 33–441 (1962).
- [34] A. N. Gent, Relaxation processes in vulcanized rubber. II. Secondary relaxation due to network breakdown, *J. Appl. Polym. Sci.* **6**, 442–448 (1962).
- [35] J. S. Bergström and M. C. Boyce, Constitutive modelling of the large strain time-dependent behaviour of elastomers, *J. Mech. Phys. Solids* **46**, 931–954 (1998).
- [36] C. Miehe and J. Keck, Superimposed finite elastic-viscoelastic-plastoelastic stress response with damage in filled rubbery polymers. Experiments, modelling and algorithmic implementation, *J. Mech. Phys. Solids* **48**, 323–365 (2000).
- [37] P. Haupt and K. Sedlan, Viscoplasticity of elastomeric materials: experimental facts and constitutive modelling, *Arch. Appl. Mech.* **71**, 89–109 (2001).
- [38] A. F. M. S. Amin, A. Lion, S. Sekita, and Y. Okui, Nonlinear dependence of viscosity in modelling the rate-dependent response of natural and high damping rubbers in compression and shear: Experimental identification and numerical verification, *Int. J. Plast.* **22**, 1610–1657 (2006).
- [39] A. Khan and H. Zhang, Finite deformation of a polymer: experiments and modelling, *Int. J. Plast.* **17**, 1167–1188 (2001).
- [40] E. Krempl and F. Khan, Rate (time)-dependent deformation behaviour: an overview of some properties of metals and solid polymers, *Int. J. Plast.* **19**, 1069–1095 (2003).
- [41] Q. Yu and A. P. S. Selvadurai, Mechanics of a rate-dependent polymer network, *Philos. Mag.* **87**, 3519–3530 (2007).
- [42] T. Heimes, Finite Thermoelastizität, (PhD dissertation, Faculty of Aerospace Engineering (University of Federal Armed Forces Munich, Neubiberg, Germany 2005).
- [43] A. N. Gent and M. Hindi, Heat build-up and blow-out of rubber blocks, *Rubber Chem. Technol.* **63**, 892 (1988).
- [44] A. Yakut and J. A. Yura, Evaluation of low-temperature test methods for elastomeric bridge bearings, *J. Bridge Eng.* **7**, 50–56 (2002).

- [45] A. Yakut and J. A. Yura, Parameters influencing performance of elastomeric bearings at low temperatures, *J. Struct. Eng., ASCE* **128**, 986–994 (2002).
- [46] D. M. Park, W. H. Hong, S. G. Kim, and H. J. Kim, Heat generation of filled rubber vulcanizates and its relationship with vulcanizate network structures, *Eur. Polym. J.* **36**, 2429–2436, (2000).
- [47] L. P. Smith, *The Language of Rubber: An Introduction to the Specification and Testing of Elastomers*, 2nd ed. (Butterworth-Heinemann, Boston, 1993).
- [48] J. P. Lin, C. Y. Chang, C. H. Wu, and S. M. Shih, Thermal degradation kinetics of polybutadiene rubber, *Polymer Degradation and Stability* **53**, 295–300 (1996).
- [49] J. A. Shaw, A. S. Jones, and A. S. Wineman, Chemo-rheological response of elastomers at elevated temperatures: Experiments and simulations, *J. Mech. Phys. Solids* **53**, 2758–2793 (2005).
- [50] A. Wineman and J. Shaw, Influence of thermally induced chemo-rheological changes on the torsion of elastomeric cylinders, *Continuum Mech. Thermodyn.* **17**, 477–492 (2006).
- [51] I. Soos, Charakterisierung des Verstärkungseffektes von Füllstoffen aufgrund der Auswertung der Spannungs-Deformations-Kurve. *GAK* **37**, 232–238, 300–303, 509–512 (1984).
- [52] A. D. Drozdov and A. Dorfmann, The influence of preloading and thermal recovery on the viscoelastic response of filled elastomers, *Mech. Res. Commun.* **29**, 247–256 (2002).
- [53] S. Govindjee and J. C. Simo, A micromechanically based continuum damage model for carbon black filled rubbers incorporating Mullins effect, *J. Mech. Phys. Solids* **39**, 87–112 (1991).
- [54] S. Govindjee and J. C. Simo, Mullins' effect and strain amplitude dependence of the storage modulus, *Int. J. Solids Struct.* **29**, 1737–1751 (1992).
- [55] S. Govindjee and J. C. Simo, Transition from micro-mechanics to computationally efficient phenomenology: Carbon black filled rubbers incorporating Mullins' effect, *J. Mech. Phys. Solids* **40**, 213–233 (1992).
- [56] M. A. Johnson and M. F. Beatty, A constitutive equation for the Mullins effect in stress controlled uniaxial extension experiments, *Contin. Mech. and Thermodyn.* **5**, 301–318 (1993).
- [57] M. A. Johnson and M. F. Beatty, Mullins effect in uniaxial extension and its influence on transverse vibration of a rubber string, *Contin. Mech. and Thermodyn.* **5**, 83–115 (1993).
- [58] R. W. Ogden and D. G. Roxburgh, A pseudo-elastic model for the Mullins effect in filled rubber, *Proc. R. Soc. Lond. A* **455**, 12861–12878 (1999).
- [59] M. F. Beatty and S. Krishnaswamy, The Mullins effect in equibiaxial deformation, *Z. Angew. Math. Phys.* **51**, 984–1015 (2000).
- [60] A. DeSimone, J. Marigo, and L. Teresi, A damage mechanics approach to stress softening and its application to rubber, *Eur. J. Mech. A, Solids* **20**, 873–892 (2001).
- [61] V. V. Moshev and S. E. Evtlampieva, Filler-reinforcement of elastomers viewed as a triboelastic phenomenon, *Int. J. Solids Struct.* **40**, 4549–4562 (2003).
- [62] D. Besdo and J. Ihlemann, Properties of rubberlike materials under large deformations explained by self organizing linkage patterns, *Int. J. Plast.* **19**, 1001–1018 (2003).
- [63] D. Besdo and J. Ihlemann, A phenomenological constitutive model for rubberlike materials and its numerical applications, *Int. J. Plast.* **19**, 1019–1036 (2003).
- [64] J. Diani, M. Brieu, and J. M. Vacherand, A damage directional constitutive model for Mullins Effect with permanent set and induced anisotropy, *Eur. J. Mech. A, Solids* **25**, 483–496 (2006).
- [65] L. Mullins and N. R. Tobin, Stress softening in rubber vulcanizates. Part I. Use of a strain amplification factor to describe the elastic behaviour of filler-reinforced vulcanized rubber, *J. Appl. Polym. Sci.* **9**, 2993–3009 (1965).
- [66] C. O. Horgan, R. W. Ogden, and G. Saccomandi, A theory of stress softening of elastomers based on finite chain extensibility, *Proc. R. Soc. Lond. A* **460**, 1737–1754 (2004).
- [67] K. R. Rajagopal and A. S. Wineman, A constitutive equation for nonlinear solids which undergo deformation induced microstructural changes, *Int. J. Plast.* **8**, 385–395 (1992).
- [68] O. H. Yeoh, Characterization of elastic properties of carbon-black filled rubber vulcanizates, *Rubber Chem. Technol.* **63**, 792–805 (1990).
- [69] Y. Yamashita and S. Kawabata, Approximated form of the strain energy density function of carbon-black filled rubbers for industrial applications, *J. Soc. Rubber Ind. (Jpn)*. **65**, 517–528 (1992).
- [70] G. Chagnon, E. Verron, L. Gornet, G. Marckmann, and P. Charrier, On the relevance of continuum damage mechanics as applied to the Mullins effect: theory, experiments and numerical implementation, *J. Mech. Phys. Solids* **52**, 1627–1650 (2004).
- [71] A. V. Tobolsky and G. M. Brown, Crystallization and relaxation of stress in stretched unvulcanized natural rubber, *J. Polym. Sci.* **17**, 547–551 (1955).
- [72] G. Kraus and J. T. Gruver, Kinetics of strain induced crystallization of a *trans*-polybutadiene, *J. Polym. Sci.* **10**, 2009–2024 (1972).
- [73] A. Wasiak, Crystallization of polymers at oriented state, *Colloid Polym. Sci.* **259**, 135–145 (1981).
- [74] J. C. Mitchell and D. J. Meier, Rapid stress-induced crystallization in natural rubber, *J. Polym. Sci. A-2, Polym. Phys.* **6**, 1689–1703 (1968).
- [75] A. N. Gent and L. Q. Zhang, Strain induced crystallization and strength of rubber, *Rubber Chem. Technol.* **75**, 923–933 (2002).
- [76] B. Lee and C. Singleton, Experimental study of the relationship of processing to the morphology in blends of SBR and cis-polybutadiene with carbon black, *J. Appl. Polym. Sci.* **24**, 2169–2183 (1979).
- [77] D. Luch and G. S. Y. Yeh, Morphology of strain induced crystallization of natural rubber. I. Electron Microscopy on uncrosslinked thin film, *J. Appl. Phys.* **43**, 4326–4338 (1972).

- [78] S. Toki, T. Fujimaki, and M. Okuyama, Strain induced crystallization of natural rubber as detected real-time by wide-angle X-ray diffraction technique, *Polymer* **41**, 5423–5429 (2000).
- [79] S. Toki, I. Sics, S. Ran, B. Hsiao, L. Liu, S. Murakami, M. Tosaka, S. Kohjiya, S. Poompradub, Y. Ikeda, and A. Tsou, Strain induced molecular orientation and crystallization in natural and synthetic rubbers under uniaxial deformation by in-situ synchrotron X-Ray study, *Rubber Chem. Technol.* **77**, 317–335 (2004).
- [80] S. Poompradub, M. Tosaka, S. Kohjiya, Y. Ikeda, S. Toki, I. Sics, and B. S. Hsiao, Mechanism of strain induced crystallization in filled and unfilled natural rubber vulcanizates, *J. Appl. Phys.* **97**, 103529-1-9 (2005).
- [81] J. Bonet, Large strain viscoelastic constitutive models, *Int. J. Solids Struct.* **38**, 2953–2968 (2001).
- [82] L. Laiarinandrasana, R. Piques, and A. Robisson, Visco-hyperelastic model with internal state variable coupled with discontinuous damage concept under total Lagrangian formulation, *Int. J. Plast.* **19**, 977–1000 (2003).
- [83] A. S. Khan, O. Lopez-Pamies, and R. Kazmi, Thermo-mechanical large deformation response and constitutive modelling of viscoelastic polymers over a wide range of strain rates and temperatures, *Int. J. Plast.* **22**, 581–601 (2006).
- [84] A. S. Khan and B. Farrokh, Thermo-mechanical response of nylon 101 under uniaxial and multi-axial loadings: Part I, Experimental results over wide ranges of temperatures and strain rates, *Int. J. Plast.* **22**, 1506–1529 (2006).
- [85] A. Escandar, M. O. Moroni, M. Sarrazin, and P. N. Roschke, Mechanical properties and fuzzy modelling of high-damping rubber with thermal effects, *J. Mater. Civil Eng., ASCE* **19**, 428–436 (2007).
- [86] P. J. Flory, Thermodynamics of crystallization in high polymers. I. Crystallization induced by stretching, *J. Chem. Physics* **15**, 397–408 (1947).
- [87] P. J. Flory, Thermodynamics of crystallization in high polymers. II. Simplified derivation of melting-point relationships, *J. Chem. Phys.* **15**, 684 (1947).
- [88] R. D. Evans, H. R. Mighton, and P. J. Flory, Thermodynamics of crystallization in high polymers. III. Dependence of melting points of polyesters on molecular weight and composition, *J. Chem. Phys.* **15**, 685 (1947).
- [89] D. E. Roberts and L. Mandelkern, Thermodynamics of crystallization in high polymers: natural rubber, *J. Am. Chem. Soc.* **77**, 781 (1955).
- [90] A. Ziabicki, Crystallization of polymers in variable external conditions. I. General equations, *Colloid Polym. Sci* **274**, 209–217 (1996).
- [91] A. Ziabicki, Crystallization of polymers in variable external conditions. II. Effects of cooling in the absence of stress and orientation, *Colloid Polym. Sci* **274**, 705–716 (1996).
- [92] A. Ziabicki, Crystallization of polymers in variable external conditions. IV. Isothermal crystallization in the presence of variable tensile stress or hydrostatic pressure, *Colloid Polym. Sci* **277**, 752–761 (1999).
- [93] A. Ziabicki and P. Sajkiewicz, Crystallization of polymers in variable external conditions. III. Experimental determination of kinetic characteristics, *Colloid Polym. Sci* **276**, 680–689 (1998).
- [94] M. Negahban, Thermodynamic modelling of the thermo mechanical effects of polymer crystallization: A general theoretical structure, *Int. J. Eng. Sci.* **35**, 277–298 (1997).
- [95] M. Negahban, Modelling the thermo mechanical effects of crystallization in natural rubber: I. The theoretical structure, *Int. J. Solids Struct.* **37**, 2777–2789 (2000).
- [96] M. Negahban, Modelling the thermo mechanical effects of crystallization in natural rubber: II. Elementary thermodynamic properties, *Int. J. Solids Struct.* **37**, 2791–2809 (2000).
- [97] M. Negahban, Modelling the thermo mechanical effects of crystallization in natural rubber: III. Mechanical properties, *Int. J. Solids Struct.* **37**, 2811–2824 (2000).
- [98] K. Kannan and K. R. Rajagopal, Simulation of fibre spinning including flow-induced crystallization, *J. Rheol.* **49**, 683–703, (2005).
- [99] K. Kannan, I. J. Rao, and K. R. Rajagopal, A thermodynamic framework for describing solidification of polymer melts, *J. Eng. Mater. Technol., ASME* **128**, 55–63 (2006).
- [100] ASTM D 832-92. Standard Practice for Rubber Conditioning for Low-Temperature Testing (American Society for Testing and Materials, PA, USA).
- [101] J. M. Chenal, L. Chazeau, Y. Bomal, and C. Gauthier, New insights into the cold crystallization of filled natural rubber, *J. Polym. Sci. B, Polym. Phys.* **45**, 955–962 (2007).
- [102] A. A. Yehia, F. M. Helaly, and S. H. Elsabbagh, Studies on mixing homogeneity of rubber blends using viscosity measurements, *J. Elast. Plast.* **24**, 15–26 (1992).
- [103] B. Jurkowska, Y. A. Olkhov, B. Jurkowski, and O. M. Olkhova, On a structure of NR and BR carbon black filled rubber compounds and vulcanizates, *J. Appl. Polym. Sci.* **75**, 660–669 (1999).
- [104] B. Jurkowska, Y. A. Olkhov, B. Jurkowski, and O. M. Olkhova, Influence of mixing procedures and curing time on molecular and topological structures of NR/BR vulcanizate, *J. Appl. Polym. Sci.* **75**, 660–669 (2000).
- [105] B. Likozar and M. Krajnc, Modelling the vulcanization of rubber blends, *Macromol. Symp.* **243**, 104–113, (2006).
- [106] S. Palaty and R. Joseph, Studies on xanthate/dithiocarbamate accelerator combination in NR/BR blends, *J. Appl. Polym. Sci.* **103**, 3516–3520 (2007).
- [107] F. Bueche, Mechanical degradation of high polymers, *J. Appl. Polym. Sci.* **4**, 101–106 (1960).
- [108] F. Bueche, Molecular basis for the Mullins effect, *J. Appl. Polym. Sci.* **4**, 107–114 (1960).
- [109] T. I. Sogolova, Super molecular structure of polymers and its effect on mechanical properties, *Mekh. Polim.* **1**, 5–16 (1965).
- [110] A. F. M. S. Amin and A. Lion, Temperature dependence of Mullins softening-healing phenomena: An outline for theoretical description based on experiments, in: *Constitutive Models for Rubber VI*, edited by G. Heinrich, M. Kaliske, A. Lion, and S. Reese (Balkema, Lisse, The Netherlands, 2009), pp. 497–503.